



HAL
open science

Thermodynamic Insights on the Feasibility of Homogeneous Batch Extractive Distillation. 1. Azeotropic Mixtures with Heavy Entrainer.

Ivonne Rodriguez-Donis, Vincent Gerbaud, Xavier Joulia

► To cite this version:

Ivonne Rodriguez-Donis, Vincent Gerbaud, Xavier Joulia. Thermodynamic Insights on the Feasibility of Homogeneous Batch Extractive Distillation. 1. Azeotropic Mixtures with Heavy Entrainer.. Industrial and engineering chemistry research, 2009, 48 (7), pp.3544-3559. <10.1021/ie801060n>. <hal-00464445>

HAL Id: hal-00464445

<https://hal.science/hal-00464445v1>

Submitted on 13 Dec 2021

HAL is a multi-disciplinary open access archive for the deposit and dissemination of scientific research documents, whether they are published or not. The documents may come from teaching and research institutions in France or abroad, or from public or private research centers.

L'archive ouverte pluridisciplinaire **HAL**, est destinée au dépôt et à la diffusion de documents scientifiques de niveau recherche, publiés ou non, émanant des établissements d'enseignement et de recherche français ou étrangers, des laboratoires publics ou privés.



HAL Authorization



Open Archive Toulouse Archive Ouverte (OATAO)

OATAO is an open access repository that collects the work of Toulouse researchers and makes it freely available over the web where possible.

This is an author-deposited version published in: <http://oatao.univ-toulouse.fr/2219>
Eprints ID : 2219

To link to this article: DOI: 10.1021/ie801060n
URL : <http://dx.doi.org/10.1021/ie801060n>

To cite this version : Rodriguez-Donis, Ivonne and Gerbaud, Vincent and Joulia, Xavier (2009) Thermodynamic Insights on the Feasibility of Homogeneous Batch Extractive Distillation. 1. Azeotropic Mixtures with Heavy Entrainer. Industrial & Engineering Chemistry Research, vol. 48 (n° 7). pp.3544-3559. ISSN 0888-5885

Any correspondence concerning this service should be sent to the repository administrator: staff-oatao@inp-toulouse.fr

Thermodynamic Insights on the Feasibility of Homogeneous Batch Extractive Distillation. I - Azeotropic Mixtures with Heavy Entrainer.

Ivonne Rodriguez-Donis¹

¹ *Instituto Superior de Tecnologías y Ciencias Aplicadas (INSTEC), Ave. Salvador Allende
Luaces, Plaza, Ciudad de la Habana,, Cuba*

Vincent Gerbaud^{2,3*} and Xavier Joulia^{2,3}

² *Université de Toulouse, INP, UPS, LGC (Laboratoire de Génie Chimique), 5 rue Paulin
Talabot, F-31106 Toulouse Cedex 01 – France*

³ *CNRS, LGC (Laboratoire de Génie Chimique), F-31106 Toulouse Cedex 01 – France*

* corresponding author : Vincent.Gerbaud@ensiacet.fr

Feasibility assessment of batch homogeneous extractive distillation for the separation of an A-B mixture feeding entrainer E traditionally relies on the systematic computation of rectifying and extractive composition profile maps under various reflux ratio and entrainer flowrate conditions. This is a well-settled methodology for determining the product sequence and the corresponding column configuration. However, we show that all related literature examples can be simply explained by using thermodynamic insights of residue curve maps, in particular, the unidistribution and univolatility curves. A general feasibility criterion at infinite reflux is proposed and finite reflux operation is also discussed. Illustration is provided for the most common cases, namely the separation with a heavy entrainer of minimum boiling (class 1.0-1a) and maximum boiling azeotropes (class 1.0-2). New cases not published so far are presented and operating conditions are also discussed. These results demonstrate the obligatory incorporation of the univolatility lines for explaining the unexpected behaviour of some particular ternary mixtures to be separated by the homogeneous extractive distillation process.

1. Introduction

The separation of azeotropic or low relative volatility (including close boiling) mixtures is a frequent challenge in many chemical processes and it can become impossible using a single conventional distillation column. Many non-conventional distillation techniques are compiled in reference monographs.¹⁻⁴ The most common alternatives involve changing the operating pressure or adding of a new compound, called entrainer. But, the pressure option is economically attractive only for mixtures very sensitive to pressure. Adding an auxiliary substance lead to azeotropic and extractive distillation processes that are carried out in a number of interconnected continuous columns or in a succession of distillation tasks in a single or in a sequence of batch distillation columns.

In batch distillation, the entrainer is always loaded initially into the still in azeotropic distillation whereas the entrainer is fed continuously in extractive distillation at some tray of the column or into the still, inducing various column configurations. When the entrainer is partially miscible with one component of the initial mixture, it is qualified as heterogeneous and the corresponding process as well. Otherwise, in azeotropic batch distillation, the first distillate (resp. bottom) product in a rectifying (resp. stripping) is the unstable/lowest boiling (resp. stable/highest boiling) node of the distillation region where the feed composition lies. However, in extractive batch distillation, a saddle/intermediate boiling point of the distillation region of the ternary diagram can be drawn as a top (or bottom) product where a non monotonous, increasing or decreasing, temperature order may occur.

Nowadays, synthesis and design of any extractive or azeotropic distillation alternative is based on the analysis of multicomponent residue curve maps⁴, whose residue curves displays all liquid composition evolution subjected to the driving force $(x - y^*)$, equal to the equilibrium vapor y^* and liquid x composition difference. Such residue curves are considered as a good approximation of the tray column liquid composition profiles under infinite reflux conditions in batch or continuous column. Under finite reflux conditions, composition profiles can be also computed using a differential mass balance⁵. Lelkes et al. have shown that batch extractive distillation synthesis and design can also be done by computing extractive composition profiles using a differential equation that also applies to azeotropic distillation.⁶

From the thermodynamic point of view, adding an entrainer (E) to a binary mixture (A-B) forms a so-called ternary diagram (A-B-E) which Serafimov classified into a finite set of 26 topologically feasible structures.⁷ So far, only 16 classes out of 26 have been matched by real ternary mixtures with significantly different occurrences.⁸ Nevertheless, batch azeotropic

distillation feasibility rules have been proposed for all 26 classes.⁹⁻¹¹ But, only four classes have been studied for batch extractive distillation.¹² They concern the separation of non ideal mixtures using homogeneous entrainers inducing no new azeotrope with the original mixture A – B. It encompasses Serafimov's 0.0-1 zeotropic class and azeotropic classes 1.0-1a; 1.0-1b and 1.0-2, representing approximately one third of occurring azeotropic mixtures.⁷

Process and operating parameters for batch homogeneous extractive distillation were reviewed for rectifying¹² and stripping column¹³. If the main process operating parameter is reflux for azeotropic distillation, the (entrainer feed/vapour flowrate) ratio is also important for extractive distillation. Column holdup and vapor flow rate (related to boiler duty) are usually less critical. Until now, the same computation methodology was used: select a diagram (A-B-E), compute composition profiles considering the batch process operating steps (infinite reflux without and with entrainer feeding, then finite reflux with entrainer feeding), and identify limiting values for reflux and entrainer flowrate. However, no general trends arose like which component is withdrawn in the distillate, the appropriate column configuration or whether limiting values of the operating parameters exist or not. Yet, in continuous extractive distillation Laroche et al. with univolatility lines and volatility order¹⁴, and Knapp and Doherty with the topological features of extractive composition profile maps¹⁵, hinted at such general trends even though they investigated mostly class 1.0-1a case; looking at the process feasibility and at the entrainer selection issue as well^{16,17} for which short cut methods were proposed.¹⁸

We intend to show in a series of manuscripts that those thermodynamic and topological features of ternary diagrams affect the synthesis and design of homogeneous extractive distillation process. Indeed, the results of Kiva et al. on the thermodynamic and topological features of ternary diagram (azeotropes, distillation boundaries defining distillation regions, elementary cells, the residue curve shape related to unidistribution lines $K_i = 1$, univolatility lines $\alpha_{i,j} = 1$, univolatility order regions)⁷ can be used, without any systematic calculations of composition profiles, to assess the feasibility of batch extractive distillation for all occurring Serafimov's classes, bringing a new light to past studies, completing some and exploring new feasible process opportunities. So, the feasibility criteria and rules that we enounce enable each time to know which component will be withdrawn in the first distillate cut, the adequate column configuration and whether a systematic study as those done so far will exhibit some limiting operating parameter value or not. Then, entrainer selection wizard tools can be devised for batch extractive distillation like those existing for batch azeotropic distillation.^{19,20}

Part I focuses on homogeneous batch extractive distillation of a minimum and maximum azeotrope binary mixture (A) – (B) where a heavy entrainer (E) alters their relative volatility without forming additional azeotropes. Part II will focus on the use of a heavy entrainer for the separation of low relative volatility mixtures. The subsequent parts will extend this analysis on the use of light and intermediate entrainer.

2. Former Studies of Homogeneous Extractive Distillation Process

Entrainer selection for homogeneous extractive distillation relies mostly on solvency, boiling point, selectivity and then thermal stability, corrosivity, toxicity, prices and other chemical properties. Solvency refers to total or partial miscibility of the entrainer with components (A) or (B). The entrainer boiling temperature sets the ternary residue curve map topology, the most appropriate column configuration and the product cut sequence. Selectivity is usually assessed via the relative volatility $\alpha_{A,B}$ and also the ratio of the activity coefficient of (A) and (B) at infinite dilution in the entrainer ($\gamma_A^\infty/\gamma_B^\infty$). The relative volatility of (A) versus (B), $\alpha_{A,B}$, is defined as the ratio of the liquid – vapour equilibrium constant K_A/K_B . Preliminary evaluation of γ_A^∞ and γ_B^∞ can be obtained by simple experimental methods or by applying adequate thermodynamics models.^{21,22}

Choosing a heavy entrainer for the separation of minimum boiling azeotropic mixtures (class 1.0-1a) is the most common industrial continuous distillation process and thus was the focus of literature study of homogeneous extractive distillation in both continuous and batch columns. To study the feasibility of continuous extractive distillation, Laroche et al. used univolatility curve ($\alpha_{A,B} = 1$) and local volatility order to determine the flowsheet of a sequence of continuous distillation columns when a light, intermediate or a heavy entrainer (E) is used for separating a minimum boiling azeotropic mixture.¹⁴ Their general feasibility criterion takes into account the interception point of the univolatility curve $\alpha_{A,B} = 1$ at the (A-E) or (B-E) side, which always starts at the original binary azeotropic composition. The residue curve inflection point line behaves similarly to the univolatility line to assess the entrainer selectivity.^{7,14,23} Separation is possible by using a direct (resp. indirect) sequence if (A) (resp. (B)) is the lightest (resp. the heaviest) component in the region where the extractive composition profile lies. Direct (resp. indirect) sequence involves a conventional continuous distillation column where the entrainer is fed above (resp. below) the main azeotropic feed. Component (A) (or (B)) is then drawn at the column top (resp. bottom) while the azeotropic binary mixture between the remaining original component and the entrainer is obtained at the opposite point of the column and separated in the subsequent distillation column. In the case

of a heavy entrainer, (A) (resp. (B)) can be distilled by using a direct sequence if the univolatility curve intercepts the (A-E) edge (resp. the (B-E) edge). The inverse case holds for a light entrainer as (A) (resp. (B)) can be recovered as the bottom product by using an indirect sequence if the univolatility curve intercepts the (B-E) edge (resp. (A-E)). With an intermediate entrainer, both alternatives are feasible: a direct sequence to obtain the light component (A) or an indirect sequence for the heavy component (B). Use of a single column for separating both components (A) and (B) as top and bottom products is also possible if a little amount of the entrainer remains inside the column. The role of the residue curve shape in this feasibility analysis was only pointed out for the case of the intermediate entrainer. Those authors also showed how such thermodynamic insights affect the entrainer selection.¹⁶

Batch extractive distillation process studies have been focused on the separation of azeotropic mixtures (minimum and maximum) and close boiling/low relative volatility mixtures. For the separation of minimum boiling mixture with a heavy entrainer (e.g. acetone – methanol with water, Serafimov's class 1.0-1a) in a batch rectifier, continuously feeding the entrainer at an intermediate tray of the batch column divides it into two sections: a rectifying section above the entrainer feed and an extractive section below it and going down to the boiler.^{24,25} For this mixture, Lelkes et al. proposed a general feasibility method consisting in finding the reflux and (entrainer feed/vapor flowrate) ratio enabling the intersection of liquid composition profile in the rectifying and extractive section, for given distillate and entrainer feed compositions.⁶ The composition profile differential model was based on a set of simplifying assumptions, infinite theoretical stages, negligible drop pressure and liquid hold-up on the trays and constant vapour and liquid overflow inside the column. The model reduces to the residue curve equation for infinite reflux and no entrainer feed.

Usually, batch extractive distillation (BED) proceeds in four operation steps: (step 1) infinite reflux operation to reach steady state inside the column, (step 2) infinite reflux operation with continuous entrainer feeding, (step 3) finite reflux leading to the distillation of one of the original component while feeding continuously the entrainer and (step 4) conventional distillation for the separation of the zeotropic binary mixture retained into the still. Step 1 feasibility obeys residue curve map analysis results as residue curve describe then the liquid composition in the column. Steps 2 and 3 are the extractive ones and their feasibility is determined by the existence of an extractive composition profile linking the rectifying profile to the instantaneous still composition, following Lelkes' model. Under feasible operating parameters, both profiles intersect close to the extractive stable node SN_{extr}

that, under high enough entrainer/vapour flowrate ratio and number of extractive tray, is commonly located near the binary side of the entrainer and the original component which is drawn as distillate product. The other azeotropic component remains into the still with the entrainer at the end of step 3.

This intersection finding methodology has been used to study the separation of minimum and maximum azeotropic mixtures and of close boiling mixtures by feeding a heavy, light and an intermediate entrainer in a batch rectifier. With rare exceptions^{16,26-28}, most papers related to batch extractive distillation have been published by Hungarian researchers group.^{6,12,13,24,25,29-38} Overall, they have considered rectifying and stripping columns and four different options for entrainer feeding: (option 1) initially with the azeotropic mixture into the still (resp. top tank) for rectifying (resp. stripping) column (SBD (resp. SBS) process), (option 2) continuously into the main tank (BED-B (resp. BES-T) process), (option 3) at an intermediate point of the column (BED-I (resp. BES-I) process) and (option 4) at the column top (resp. bottom) for rectifying (resp. stripping) column (BED-T (resp. BES-B) process). Therefore, the column has a single rectifying (resp. stripping) section for rectifying (resp. stripping) column (option 1 and 2) or an extractive section (option 4) or two sections, rectifying (resp. stripping) and extractive, for rectifying (resp. stripping) column (option 2). Using the differential model of Lelkes et al. for a rectifier column⁶ and of Varga for a stripper column.¹³, those authors systematically calculated composition profile maps in each column section under various process operating conditions and they were able to assess the feasibility of all eight column configurations cited above during the process steps and evaluate the occurrence of limiting values for the reflux, for the (entrainer feed/vapour flowrate) ratio, and for the number of stages in the various column sections.^{12,13} Comparison of all processes lead to recommend the use of BED-I or BES-I column configurations¹³ and they are the two configurations we consider as well.

3. Thermodynamic Topological Structures for Homogeneous Extractive Distillation Processes.

For the separation of a minimum or of a maximum boiling azeotrope or of a low relative volatility mixture by using a light, intermediate or heavy entrainer adding no new azeotrope, Table 1 and Figure 1 display the ternary diagram classes associated to the homogeneous extractive distillation process. Note, that antipodal structure is applied for the maximum boiling azeotrope from the minimum azeotropic one and vice versa. The low volatility mixture is represented by the ternary zeotropic mixtures 0.0-1.

Hilmen et al. reported the occurrence in Reshetov's statistics of the 26 ternary diagram classes and established that all can be represented by a combination of four elementary cells, which display one unstable $[UN_{rcm}]$ and stable $[SN_{rcm}]$ node number and one or several saddle points $[Sr_{cm}]$ as singular points of the residue curve map.⁸ More than 90% of the reported ternary diagrams involve two elementary cells triangular I and rhombic II containing one and two saddle points, respectively. In both cells, a residue curve ends at the stable node passing through a single saddle point from the unstable node (see Figure 1). In cell I, the residue curve follows a sole path due to the presence of one saddle point but can have either a S-shape or a C-shape. Cell II exhibits two opposite saddle points and the residue curve can reach the stable node by two different paths (see Figure 1). Until now, feasibility of the non conventional distillation process is based on the analysis of the entire ternary diagram. Occurrence of S-shape or of C-shape residue curve is later shown for class 1.0-2 to affect the feasible region size and product recovery.

Ternary diagram class 1.0-1a contains the elementary cell II and corresponds to the popular extractive distillation industrial case (minimum boiling azeotrope with a heavy entrainer or maximum boiling azeotrope with a light entrainer). Its occurrence is among the top three most common structures (21.6%). Diagram 1.0-2 concerns minimum boiling azeotrope with a light entrainer or maximum boiling azeotrope with a heavy entrainer. It contains two elementary cells I and has only 8.5% of reported occurrence. More frequently, a light entrainer used for the separation of a minimum boiling azeotrope will add a new azeotrope with the lightest original component (A) leading to the frequent class 2.0-2b diagram composed by two elementary cells I and II (occurrence 21.0%).⁸ Related to the use of an intermediate entrainer, diagram 1.0-1b is among the rarest (occurrence 0.4%) and has a single elementary cell III. Maximum boiling azeotropes are less abundant in nature than minimum boiling temperature mixtures according to experimental data.³⁹

Even the zeotropic ternary diagram 0.0-1 prediction of feasible distillation product composition for a specified column configuration is not simple because there might exist different volatility order regions within composition space that can change the simple phase transformation path. Indeed, separation of the unstable (stable) pure component in a rectifying (stripping) column is an impossible task because the residue curve exhibits an inflection point caused by the existence of at least one univolatility line. Kiva et al.⁷ showed that the presence of any univolatility line changes the volatility order of the components in any ternary mixtures 123. They showed how a combined diagram of unidistribution ($K_i = 1$) and univolatility lines

($\alpha_{i,j} = 1$) enables to sketch the residue curve map without any calculation. Inflexion point of the residue curve occurs at the univolatility line if there is no unidistribution line between the univolatility line and the stable or unstable node linked by the corresponding residue curve that has a so-called S-shape. This general behavior was illustrated for several ternary mixtures for Serafimov's classes 0.0-1, 1.0-1a, 1.0-1b, 1.0-2, 1.1-2, 2.0-1, 2.0-2a, 2.0-2b, 2.0-2c, 3.0-2, 3.1-2 and 3.1-3b.⁷

As pointed out before, the univolatility line has not been considered to its full extend for the synthesis and design of homogeneous extractive distillation process in all nine possible cases described in Table 1. Only, Laroche et al. and Pöllmann and Blass used this concept or residue curve inflexion line to determine the continuous column configuration and the component to be drawn as the first top or bottom product for separating minimum boiling azeotropes.^{14,23} In subsequent works concerning batch distillation, the role of univolatility line has been hinted at, but the feasibility of the process is mainly determined by computing the liquid composition profile in each column section.^{6,12,13,24,25,29-38} Because the univolatility line characterizes the liquid-vapour equilibrium behavior of any ternary mixture, a general feasibility criterion can be established combining the topology of the residue curve map and the information about the region of the composition space with different volatility order of the components.

4. Feasibility Criterion for the Synthesis of Homogeneous Extractive Distillation Processes in Batch Column

The general feasibility criterion for homogeneous extractive distillation process in a rectifier or stripper batch column under infinite reflux condition is based on residue curve map analysis together with the occurrence of any univolatility line. Hence, the first product cut component and the column configuration based on the thermodynamic nature of the ternary mixture can be predicted without any computation, following a methodology similar to that used for batch azeotropic distillation process.^{9,11,40} The influence of finite reflux on this criterion is discussed afterwards. The general criterion under infinite reflux operation states that *“homogeneous batch extractive distillation of a (A) – (B) mixture with entrainer (E) feeding is feasible if there exists a residue curve connecting (E) to (A) or (B), following a decreasing (a) or increasing (b) temperature direction inside the region where (A) or (B) is the most volatile (a) or the heaviest (b) component of the mixture”*.

Figure 2 details the unidistribution ($K_i = 1$) and univolatility lines ($\alpha_{i,j} = 1$) occurring in the ternary diagrams corresponding to the four classes reported in Table 1.⁷ The simplest class

0.0-1 corresponds to low relative volatility mixture where each type of entrainer (light; intermediate and heavy) is set as component (1), (2) and (3) in the ternary diagram of Figure 2(a). Reshetov and Kravchenko published statistics of the 15 experimentally reported ternary zeotropic mixtures among 33 possible zeotropic classes. The simplest zeotropic class with no univolatility line occurrence is 71.6%, while four other classes with a single univolatility line, either α_{12} or α_{23} , add up to 26.4% of reported diagrams.⁴¹

For class 0.0-1, there is one unidistribution line related to the saddle intermediate boiling component (K_2). Two univolatility curves (α_{12} ; α_{23}) may arise, often one at each time and located between the saddle point and the unstable and stable node changing the component volatility order in the composition space. Despite the absence of azeotropic point in these diagrams, either α_{12} or α_{23} affect the separation of such zeotropic mixture by using light, intermediate or heavy homogeneous entrainer.⁴²

Azeotropic ternary diagrams 1.0-1a, 1.0-2 and 1.01b are displayed with components (1) and (2) being the azeotropic ones, ((1) lighter than (2)) and, (3) being the entrainer. Ternary diagram 1.0-1a is displayed in Figure 2b. It concerns the separation of minimum (resp. maximum) boiling azeotropes with a heavy (resp. light) entrainer. Two unidistribution lines (K_1 , K_2) related to the azeotropic components occur, starting at the (1-2) azeotrope and ending at the pure component vertex. The univolatility curve α_{12} is always present but has two alternative locations. It starts at the azeotrope and ends at the binary side limited by the entrainer and either the light (1-3) or the heavy azeotropic component (2-3). The precise ending location sets the first product cut. Two other univolatility curves α_{23} and α_{13} can also occur and are located on the binary azeotropic side close to the pure component (1) and (2), respectively because they can not cross the unidistribution lines.

As Figure 2b shows, univolatility lines set regions with different volatility order. Component (1) (resp. (2)) is more volatile than (2) (resp. (1)) above (resp. below) the univolatility line α_{12} . Notice that this holds whatever the occurrence of α_{13} and α_{23} curves.

Ternary diagram 1.0-2 (Figure 2c) exhibits a similar behavior with two unidistribution lines K_1 , K_2 and up to three univolatility curves α_{12} , α_{13} and α_{23} . Unidistribution lines K_1 , K_2 begin at the azeotrope and end at the opposite binary side (2-3) and (1-3), respectively. α_{12} starts at the azeotrope and ends at the binary side limited by the entrainer and either the light or the heavy azeotropic component. The univolatility line α_{12} changes the volatility order between the azeotropic components in both regions. If present, α_{13} or α_{23} forms a semicircle on the

binary side of the azeotropic components (1-2) (similar to Figure 2b) or around the vertex of original component (2) and (1), respectively (see Figure 2c). Up to four volatility order regions may then occur.

Diagram 1.0-1b (Figure 2d) concerns the separation of minimum or maximum boiling azeotropes using intermediate entrainers. Three unidistribution lines (K_1, K_2, K_3) and three univolatility curves α_{12} , α_{13} and α_{23} may occur. In the case of a minimum (resp. maximum) boiling azeotrope, α_{12} starts at the binary azeotrope and ends at the binary side (1-3) (resp. (2-3)) limited by the entrainer and the light (resp. heavy) azeotropic component. A second univolatility line α_{23} (resp. α_{13}) always exists and it is parallel to the corresponding binary side (2-3) (resp. (1-3)). Occasionally, α_{13} (resp. α_{23}) occurs on the binary side of the azeotropic components close to both vertices avoiding the interception of the unidistribution lines K_1 (resp. K_2) and K_3 . Five volatility order regions may be found.

5. Topological features related to process operation of minimum boiling azeotrope separation with a heavy entrainer by batch homogeneous extractive rectification (class 1.0-1a)

The general feasibility criterion enounced above strictly holds for infinite reflux operation, corresponding to step 1 and 2 of the batch extractive distillation process. For finite reflux (step 3), things are more complicated and can only be exhaustively studied from the computation of extractive singular points as was done for the minimum boiling azeotrope separation with a heavy entrainer (class 1.0-1a) by batch homogeneous extractive rectification (BED process).⁴³ Figure 3 displays the qualitative topological features of the class 1.0-1a diagram. These are adapted from both Knapp and Doherty study in the continuous column using a stage by stage model¹⁵ and Frits et al. study of the batch process.⁴³ using the differential model of Lelkes et al.⁶ and combined with insights from Laroche's work using the univolatility curve $\alpha_{AB} = 1$.¹⁴

Initially, the still is loaded with the T_{\min} azeotrope. Pure entrainer (E) is fed in the middle of the column defining an extractive section below the feed and a rectifying one above. Depending on the so-called reflux ratio R ($R = \text{reflux}/\text{distillate flowrates}$) and on the (entrainer feed/vapor flowrates) ratio (F_E/V), composition profiles can be computed using the general differential model of Lelkes et al. once a distillate composition x_D has been chosen⁶:

$$\frac{dx_i}{dh} = \frac{V}{L}(y_i - y_i^*) \quad (1)$$

where h is the dimensionless column height; V and L are the vapor and liquid flowrates, respectively; y_i^* is the vapor composition in equilibrium with the liquid composition x_i and y_i is computed from a component molar balance involving the external streams: entrainer supply F_E and distillate withdrawal D .¹²

$$\frac{V}{L} = \frac{V}{V + F_E - D} = \frac{R + 1}{R + (R + 1) \cdot (F_E / V)} \quad (2)$$

$$y_i = \frac{(V + F_E - D)x_i + Dx_D - F_E x_E}{V} = \left(\frac{R}{R + 1} + (F_E / V) \right) x_i + \frac{1}{R + 1} x_D - (F_E / V) x_E$$

Similarly, the still composition is determined by equation (3)

$$\frac{d(Ux_s)}{dt} = F_E x_E - Dx_D \quad (3)$$

Through the manuscript, all composition maps are computed from these equations using Simulis Thermodynamics® property server package and services available in Excel.⁴⁴

Feasible and unfeasible regions for the composition in the extractive section of the column are deduced from the analysis of the extractive composition profile map, similarly to residue curve map (rcm) analysis. Those regions are bounded by extractive stable and unstable separatrices crossing at saddle extractive singular points.¹⁵ For the class 1.0-1a, the pinch point of the extractive composition profiles is a stable extractive node SN_{extr} issued from the original minimum boiling azeotrope. Saddle extractive points $S_{i,extr}$ are emerged from the rcm saddle points (A and B vertices). An extractive unstable node UN_{extr} is located at the entrainer vertex. We now discuss Frits et al. conclusions in the perspective of univolatility concept.⁴³

At infinite reflux with no entrainer feeding (BED process step 1), rcm holds (Figure 3a). The column has a single rectifying section which composition profile in a tray column follows strictly a residue curve assuming constant molar overflow hypothesis and infinite number of trays.⁴ Rcm analysis states that the minimum boiling azeotrope, being the unique rcm unstable node, is obtained at the column top.

At infinite reflux, as soon as the entrainer feed ratio is turned on ($F_E/V \rightarrow 0^+$) (BED process step 2), two column sections occur, a rectifying one above the feed and an extractive one below. The rectifying section composition profiles are residue curves as in Figure 3a. Figure 3b sketches the extractive composition profiles map. Extractive singular points have the opposite stability of the rcm singular points by comparing Figure 3a and 3b as explained in the literature.¹⁵ Of utmost importance is the univolatility curve $\alpha_{AB} = 1$ that starts at the azeotrope $T_{\min} \text{ azeo}_{AB}$ and intersects the (A-E) edge at x_P . The general criterion we have

enounced previously holds for (A) that is then the first product cut of the BED process provided that an adequate reflux and entrainer flowrate values are set. Note that as (A), (B) and (E) are extractive singular points, the (A-E), (B-E) and (A-B) edges are respectively unstable, unstable and stable extractive separatrices.

At infinite reflux while F_E/V increases (Figure 3c), SN_{extr} moves along $\alpha_{AB} = 1$, $S_{A,extr}$ and $S_{B,extr}$ moves along the binary edges (A-E) and (B-E), respectively, towards the (E) vertex which makes the entrainer. Extractive stable separatrices linking $SN_{extr} - S_{A,extr} - S_{B,extr}$ move inside the composition triangle towards (E) with no effect on feasibility.

Close to a limiting value $F_E/V_{min,R\infty}$, SN_{extr} and $S_{A,extr}$ merge and the extractive composition profiles are attracted to a new extractive stable node SN'_{extr} located below the (A-E) edge. $F_E/V_{min,R\infty}$ is defined as the value for which the process becomes feasible: extractive composition profiles ending at SN'_{extr} cross a rectifying profile that can reach the vicinity of the expected product (A) (Figure 3d).

At finite reflux ratio with $F_E/V = 0$, finite residue curve shapes are altered.⁴⁵ Besides, singular points move inside or outside the ternary diagram and separatrices arise. At high finite reflux, rectifying profiles follows approximately a residue curve shape. At very low reflux ratio, their length can be shortened by a pinch, not joining the rcm unstable node to the rcm stable node.¹³

At finite reflux ratio with $F_E/V \rightarrow 0^+$ (Figure 3e), SN_{ext} no longer belongs to the univolatility curve but starts closer to (B) on the (B- $T_{min}Azeo_{AB}$) segment and moves inside the triangle along with the both saddles $S_{A,extr}$ and $S_{B,extr}$. The stable extractive separatrices $S_{A,extr} - SN_{extr}$ and $S_{B,extr} - SN_{extr}$ are the sequel of the (A-B) edge moving inside the triangle. UN_{extr} also moves slightly inside and sets with $S_{A,extr}$ and $S_{B,extr}$ two extractive unstable separatrices with significant curvature. Those separatrices end outside the triangle towards unstable nodes UN'_{extr} and UN''_{extr} . They are the sequel of the (A-E) and (B-E) edges, extractive unstable separatrices at infinite R , moving inside the triangle at finite reflux (Figure 3e)

As F_E/V increases at finite R , the extractive unstable separatrix $UN_{extr} - S_{A,extr} - UN''_{extr}$ near the (A-E) edge quickly disappears (see Figure 3e). In the meanwhile (Figure 3f), $S_{B,extr}$ moves towards the E vertex inside the triangle. Consequently, the extractive unstable separatrix $UN_{extr} - S_{B,extr} - UN'_{extr}$ remains. Besides, the extractive stable separatrix also stays joining $S_{B,extr}$ to SN'_{extr} and SN''_{extr} located outside the ternary composition space through the (B-E) edge. At finite reflux, there exists $F_E/V_{min,R>0} > F_E/V_{min,R\infty}$ above which SN_{extr} and $S_{A,extr}$ have

merged and the extractive composition profiles are attracted to a new extractive stable node SN'_{extr} located below the (A-E) edge (Figure 3f).⁴³ This enables to connect the still composition via a composite extractive and rectifying profile to the vicinity of (A) and the process becomes feasible again. But, the extractive unstable separatrix $UN_{extr} - S_{B,extr} - UN'_{extr}$ remains and now sets unfeasible composition regions (I and II) located above it (see Figure 3f) that prevent the total recovering of component (A) from the column. Notice also that there exists a minimum reflux ratio R_{min} at a given F_E/V , for which the still composition path lies entirely inside the unfeasible regions I or II. This condition is accomplished when the unstable separatrix $UN_{extr} - S_{B,extr} - UN'_{extr}$ is tangent to the still path.

So finite reflux operation is feasible if $F_E/V > F_E/V_{min,R>0}$ and $R > R_{min}$. Now, as (E) is fed to the column, the composition profile moves towards (E) and away from the distillate that is close to (A) (see Figure 3f). Besides, the size of the unfeasible region increases as R decreases. So recommended operation is to start at low reflux and increase reflux ratio preventing the column composition (or still path) to cross the unstable separatrix $UN_{extr} - S_{B,extr} - UN'_{extr}$ and lie inside the unfeasible region.

Differential profiles do not hint at the number of theoretical trays in each column section. In practice, if the number of theoretical trays in each column section is large enough, composition profiles reach close enough to their nodes. So, there exists a minimum number of theoretical trays in both section and also a maximum in the rectifying section. Indeed, the residue curve starts at the T_{min} azeotrope AB and too many rectifying trays would force the rectifying profile to approach to (A) (expected product) but, then turn away from (A) towards the T_{min} azeotrope AB.

In summary, we state that *a priori* knowledge of the residue curve shape and the location of the univolatility curve $\alpha_{AB} = 1$ intersection with a diagram edge enables to predict the distillate product obtained by extractive distillation as first cut. Secondly, the existence of an unstable separatrix (coming from an extractive saddle opposite to the distillate) must be tracked down as it sets an unfeasible composition region that prevents total product recovery under finite reflux operation.

6. Separation of Azeotropic Mixtures by Homogeneous Extractive Distillation in a Batch Rectifying Column.

6.1. Separation of Minimum Boiling Temperature Azeotropes with Heavy Entrainers (class 1.0-1a).

Figure 4 displays the ternary diagram 1.0-1a. From Figure 2, $\alpha_{AB} = 1$ intersect the binary side between the entrainer (E) and either the light (A) or the heavy original component (B). Rcm topological characteristics are the same for both cases as we discussed above (compare Figure 4a and 4b).

Separation of T_{\min} azeotrope AB by using an azeotropic distillation process in a batch rectifier or batch stripper is not achievable because the general feasibility criterion for azeotropic distillation enounced by Bernot et al. is not matched as both (A) and (B) are saddles and they are located in different batch distillation regions.⁴⁶ As Figure 4 shows, residue curves begin at the unstable azeotropic point and end at the stable entrainer vertex (E) following two different trajectories depending on the saddle point (A or B). From (E) towards (A) or (B) temperature decreases along the residue curve. Therefore, theoretically both azeotropic components can be distillated first in a batch extractive rectifier with a finite number of theoretical stages.⁶ What component is really drawn as first distillate cut depends on what binary side (A-E) or (B-E) intercepts the univolatility curve $\alpha_{AB} = 1$ for extractive distillation process in a rectifying column.

In case *a* (Figure 4a), $\alpha_{AB} = 1$ reaches the binary side (A-E) dividing the diagram in two volatility order regions, (A) being more volatile than (B) in the region located in the left side of α_{AB} . So according to the new extractive feasibility criterion, the region where temperature decreases from (E) to the product and the product is the most volatile concerns component (A). Hence, component (A) is the first distillate cut.

In case *b* (Figure 4b), the region where temperature decreases from E to the product and the product is the most volatile concerns component (B) and (B) is the first distillate product.

For both cases, feasible rectifying and extractive liquid profiles intercept inside the feasible region at point SN_{extr} , close to the (A-E) (case *a*) or (B-E) (case *b*) edge. SN_{extr} (strictly speaking SN'_{extr} , see previous section) is always located near the segment of the residue curve $[x_P; (E)]$ where x_P is the interception point between the univolatility curve and residue curve passing through the selected distillate composition for (A) or (B). Separation of (A) (case *a*) or (B) (case *b*) at the column top takes place using the minimum amount of entrainer $(F_E/V)_{\min}$ if $SN_{A,extr}$ (case *a*) or $SN_{B,extr}$ (case *b*) coincides with x_P . The influence of R and F_E/V was recalled in the previous section (see Figure 3) and the dragging of the extractive unstable separatrix inside the diagram prevented from recovering all component (A).

Below examples are presented with thermodynamic models and parameters given in Table 2.

6.1.1. Class 1.0-1a, Case a: $\alpha_{AB} = 1$. Curve reaching the binary side (A-E). An exhaustive parametric study of case *a* using a rectifier was published considering the separation of acetone – methanol using water as homogeneous entrainer.^{6,12} Laroche et al. used ethanol or isopropanol as heavy entrainers instead of water for the continuous process.¹⁴

Indeed, continuous and batch processes obey the same feasibility criterion enounced in section 5. For example, let's consider the batch separation of the minimum boiling azeotropic mixture acetone (A) – heptane (B) by using toluene (E) as proposed by Laroche et al. using a continuous extractive distillation process.¹⁴ Figure 5a displays the thermodynamic behavior of this ternary mixture matching those showed in Figure 4a. As expected from the extractive criterion, acetone is first removed in the distillate. A rectifying and an extractive composition profile are shown in Figure 5a for two F_E/V values under infinite reflux and with $x_{DA}^{acetone} = \{0.950, 0.025, 0.025\}$, where the component position in the composition vector was defined considering the decreasing boiling temperature order ($A < B < E$). This notation will be used hereafter. For $F_E/V = 0.05 < (F_E/V)_{min} = 0.1$, SN_{extrA} is located on the univolatility line. For $F_E/V = (F_E/V)_{min}$, SN_{extrA} coincides with x_P point, that is the interception point between the univolatility line α_{AB} and the residue curve at infinite reflux passing through x_{DA} . For $F_E/V = 0.2 > (F_E/V)_{min}$ (Figure 5b) the whole ternary composition space matches the feasible region as all extractive composition profiles end at the stable node SN'_{extrA} . Figure 5b shows an extractive composition profile maps similar as in Figure 3d: the binary extractive saddle $S_{B,extr}$ comes from the saddle heptane vertex and alters the extractive composition profiles curvature close to the binary side heptane – toluene. Besides, there exists an extractive stable separatrix linking $S_{B,extr}$ to SN'_{extrA} and an extractive unstable node (UN_{ext}) located at the toluene vertex under infinite reflux ratio.

Under finite reflux ratio, as predicted, the key features are that $S_{B,extr}$ and the extractive unstable separatrix $UN_{extr} - S_{B,extr} - UN'_{extr}$ move inside the diagram as shown for $F_E/V = 0.2$ and $R = 5$ (Figure 6). An unfeasible composition region happens as any extractive composition profile on the left of the extractive unstable separatrix reaches the binary side heptane – toluene and doesn't intercept any rectifying profile leading to the expected distillate near (A). As stated, the extractive unstable separatrix sets a boundary that the still path should not cross. Therefore, process operation should start with a low reflux and as the still composition closes the extractive unstable separatrix, reflux should be increased to move back the extractive unstable separatrix $UN_{extr} - S_{B,extr} - UN'_{extr}$ towards the heptane – toluene edge where it lies at infinite reflux.

6.1.2. Class 1.0-1a, case b: $\alpha_{AB} = 1$. Curve reaching the binary side (B-E). Class 1.0-1a case *b* (Figure 4b) examples where the original heavy component (B) is distilled first are scarce in the literature. Laroche et al. proposed the separation of acetone – methanol with chlorobenzene as heavy entrainer by using a continuous distillation column.¹⁴ Again, batch operation runs as well. Figure 7a shows that the univolatility curve $\alpha_{AB} = 1$ reaches the binary side methanol (B) - chlorobenzene (E). (E) and (B) as well as (E) and (A) are connected by a residue curve in the decreasing temperature direction. Targeting a distillate of $x_{DB} = \{0.025, 0.9500, 0.025\}$, the residue curve going through x_{DB} is a good approximation of the rectifying liquid composition profile. Below $\alpha_{AB} = 1$ where (A) lies, methanol (B) is the most volatile component and a decreasing temperature residue curve goes from (E) to (B). According to the extractive criterion, it is also the feasible region enabling to recover (B). That criterion does not hold for (A) in the region above $\alpha_{AB} = 1$.

Figure 7a shows that for $F_E/V \leq (F_E/V)_{min} = 0.6$, the extractive composition profile stable node SN_{extrB} moves away from the T_{min} azeo_{AB} along the univolatility line until it intersects at the so-called point x_P the rectifying profile enabling to reach x_{DB} at $(F_E/V)_{min} = 0.6$. For $F_E/V = 1 > (F_E/V)_{min}$ (Figure 7b), all extractive composition profiles finish at SN'_{extrB} close to the (B-E) edge, but on the $[x_P; (E)]$ segment side. As F_E/V increases, UN_{extr} lies in (E) and a $S_{A,extr}$ saddle has moved from (A) towards (E) along their respective triangle edge. The (A-E) edge is indeed an extractive unstable separatrix with no consequence on the feasibility under infinite reflux.

However, under finite reflux conditions, the saddle $S_{A,extr}$ moves inside the triangle and drags along the extractive unstable separatrix $UN_{extr} - S_{A,extr} - UN'_{extr}$. It generates an unfeasible composition region that grows as the reflux ratio decreases. Figure 8 displays the map of extractive composition profiles for $F_E/V = 1$ and $R = 10$ and shows this behavior that has not been published so far for case *b* of Figure 4. The region located below the extractive unstable separatrix becomes unfeasible for separating methanol because the extractive composition profile reaches SN_{extrA} instead of SN_{extrB} . The extractive unstable separatrix also restricts the recovery of methanol because it prevents the still path to end at the acetone – chlorobenzene edge.

Figure 8 also shows the rigorous simulation results using ProSim Batch.⁴⁴ An equimolar mixture is considered as initial charge into the reboiler (x_{S0}) of a column with 50 theoretical trays. A distillate purity for methanol, $x_{DB} = \{0.01, 0.98, 0.01\}$ is targeted. Chlorobenzene is fed at tray 5 counting from the top. The vapour flowrate provided by the reboiler and the

entrainer flowrate are set in order to obtain approximately $F_E/V = 1$ inside the extractive column section. The still path and the liquid profile inside the column during the key operating steps are displayed in Figure 8. During step 1 (infinite reflux without entrainer feeding), the rectifying liquid profile reaches the rcm unstable node acetone – methanol azeotrope x_{azeo} . Entrainer feeding at infinite reflux (step 2) shifts the still composition towards the chlorobenzene entrainer vertex. Rectifying and extractive sections liquid composition profiles are shown in Figure 8 for the still composition x_{SJ} . Both column section profiles intercept close to SN_{extrB} as predicted and the rectifying profile meets the x_{DB} target. Therefore, a methanol rich distillate can be withdrawn instead of the original binary azeotrope at the column top thanks to the continuous feeding of chlorobenzene in the further step 3 under finite reflux ratio conditions. For $R = 10$ (Figure 8), the still path at x_{SJ} is influenced by both the pure entrainer feeding (x_E) and the distillate withdrawal x_{DB} (see equation 3). At the end of step 3, methanol recovery is almost complete because the still path finishes very close to the binary side acetone – chlorobenzene (x_{SJ}) despite the presence of the extractive unstable separatrix located almost on the acetone – chlorobenzene edge for $x_{chlorobenzene} > 0.9$.

6.2. Separation of Maximum Boiling Temperature Azeotropes with Heavy Entrainers (class 1.0-2)

Figure 9 displays the ternary diagram 1.0-2 concerning the separation of maximum boiling azeotropes using heavy entrainers. From Figure 2, $\alpha_{AB} = 1$ intersect the binary side between the entrainer (E) and either the light (A) or the heavy original component (B). Residue curve map topology is the same for both cases: both original components (A) and (B) are unstable nodes; the entrainer (E) is the stable node while the maximum boiling azeotrope $T_{max} azeo_{AB}$ is a saddle point. The rcm stable separatrix, also called basic distillation region boundary links the azeotrope to (E). Separation of (A) and (B) is theoretically not possible by conventional azeotropic distillation adding (E) initially into the still because (A) and (B) are located in different distillation regions separated by the rcm stable separatrix. But, azeotropic batch distillation was feasible for the ternary system acetone (A) – chloroform (B) – benzene (E) (Figure 9a) thanks to the curvature of the stable separatrix.^{45,47} Later, Lang et al. showed for this mixture that batch extractive distillation also performs well^{31,32}, using the simplified feasibility method of Lelkes et al.⁶ Comparing azeotropic and extractive batch distillation, they showed that extractive distillation performed better than azeotropic because the feeding of entrainer generates an extractive separatrix also curved and closer to the (B-E) side than the rcm stable separatrix, thus increasing the feasible region in which (A) is the unstable node.

Hence, the extractive distillation alternative improves the recovery yield of component (A) as first distillate cut.

In case *a* (Figure 9a), $\alpha_{AB} = 1$ reaches the binary side (B-E) and defines two volatility order regions, (A) being more volatile than (B) in the region containing (A) vertex. Case *b* (Figure 9b) is analogous to case *a*, but for $\alpha_{AB} = 1$ curve that intercepts the binary side (A-E).

According to the feasibility criterion proposed at infinite reflux, the region where temperature decreases from (E) to the product and the product is the most volatile, concerns now both (A) and (B). So, for class 1.0-2, both (A) or (B) can be drawn as first distillate cut of homogeneous extractive distillation. Nevertheless, both potential distillates are not subject to the same operating conditions. At $F_E/V = 0$, SN_{extrA} (resp. SN_{extrB}) coincides with (A) (resp. (B)). Thus at $F_E/V = 0$, either (A) or (B) can be recovered; by azeotropic distillation; because they are already the unstable node of the region where they are the most volatile component. Therefore, unlike class 1.0-1a where both original components are saddles; extractive operation with continuous feeding of the entrainer at an intermediate column point under infinite reflux is not imperative for class 1.0-2 diagram where both original components are unstable nodes.³¹

As seen in Figure 9 case *a*, if there is no F_E/V limit to recover (A), there exists a maximum value $(F_E/V)_{max,B,R\infty}$ to recover (B) due to the interception of the univolatility line $\alpha_{AB} = 1$ with the (B-E) edge. However, below $(F_E/V)_{max,B,R\infty}$, composition region restriction apply to recover a specific product. Similarly in Figure 9 case *b*, a $(F_E/V)_{A,MAX,R\infty}$ exists to recover (A) and no entrainer flowrate restrictions apply to recover (B).

The existence of maximum or minimum entrainer flowrate value depends then on the occurrence of univolatility lines under infinite reflux operation. Determination of their precise values requires computation of extractive profiles nodes location, either from extractive profile maps, as we do or from finding the roots and turning points of the differential set of equation by interval analysis¹⁵ or by bifurcation analysis⁴³.

Further insights on class 1.0-2 extractive distillation are evident if we recall the key features of class 1.0-1a (see Figure 3 and related section), namely that first under infinite R and $F_E/V \rightarrow 0^+$, rcm stability of the singular points is reversed for the extractive profile map (Figure 3b). Second, the occurrence of an unstable extractive separatrix prevents complete recovery of distillate as an unfeasible region arises, of growing size as R decreases.

Applied to class 1.0-2, under infinite R and $F_E/V \rightarrow 0^+$, the maximum boiling azeotrope azeo_{AB} is a saddle S_{extr} , (A) and (B) are stable extractive nodes $SN_{extr,A}$ and $SN_{extr,B}$ whereas (E) is an unstable extractive node UN_{ext} . There will always be an unstable extractive separatrix between UN_{ext} (E vertex) and S_{extr} (T_{\max} azeo_{AB}). As $F_E/V > 0^+$ and infinite R , S_{extr} moves inside the ternary composition space, precisely along the univolatility line α_{AB} . Furthermore, the stable extractive nodes, $SN_{extr,A}$ and $SN_{extr,B}$, move towards (E) over the binary edges (A-E) and (B-E), respectively. Therefore, a stable extractive separatrix $SN_{extr,B} - S_{extr} - SN_{extr,A}$ and an unstable extractive separatrix $UN_{ext} - S_{extr} - UN'_{ext}$ similar to those shown in Figure 3f exist even for infinite reflux ratio. Logically, under finite reflux ratio, the unstable extractive separatrix $UN_{ext} - S_{extr} - UN'$ will move towards the selected distillate product (A) or (B) reducing the size of their respective feasible region. All these general features of the topology of the extractive composition profile map and its difference with class 1.0-1a are now discussed depending on the $\alpha_{AB} = 1$ curve interception with the triangle edges.

6.2.1 Class 1.0-2 case a: $\alpha_{AB} = 1$. Curve reaching the binary side (B-E). Batch extractive distillation of acetone (A) – chloroform (B) with benzene (E) as heavy homogeneous entrainer studied by Lang et al. is now revisited for illustration.^{31,32} The corresponding residue curve map is shown in Figure 10a. Two univolatility lines, α_{AB} and α_{BE} , exist in the ternary system defining three volatility order regions. $\alpha_{AB} = 1$ line intercepts the binary side chloroform (B) – benzene (E). Below (resp. above) $\alpha_{AB} = 1$, acetone (A) (resp. chloroform (B)) is the most volatile component, respectively. The other univolatility line α_{BE} affects only (B) and (E) relative volatility but does not affect (A) and (B) relative volatility and has no incidence for the product cut prediction.

Two rectifying profiles are computed for two potential distillates, either rich in acetone (A) or in chloroform (B) such that $x_{DA} = (0.9900, 0.0001, 0.0099)$ and $x_{DB} = (0.0001, 0.9900, 0.0099)$. Due to the highly curved separatrix, a significant deviation of the rectifying profile is produced by increasing slightly the amount of chloroform (B) (resp. acetone (A)) in x_{DA} (resp. x_{DB}). Figure 10b displays the extractive composition profile map for $(F_E/V) = 0.05$ under infinite reflux ratio. Extractive singular points and separatrices behave as described above. The extractive unstable separatrix links S_{extr} with the node UN_{ext} (E vertex) and a point x_{AB} located on the binary side acetone – chloroform, having an acetone composition of 0.33 approximately.

Regions I and II are feasible for recovering distillate (B) because for any still composition inside, an extractive profile reaches $SN_{extr,B}$ that is connected to x_{DB} by a rectifying profile of

decreasing temperature from (E) to (B). Symmetrically, regions III and IV are feasible for recovering distillate (A). The unstable extractive separatrix $UN_{extr} - S_{extr} - x_{AB}$ is located above the typical rcm stable separatrix that is entirely contained in regions III and IV.

Figure 11a shows the extractive composition profile maps for a higher value of $F_E/V = 0.2$ while R is infinite. The feasible region size for distillate (A) (region III and IV) has increased as S_{extr} moves on $\alpha_{AB} = 1$ towards x_P and $x_{AB} \cong 0.18$ moves closer to (B). Further increase of F_E/V allows the fusion of S_{extr} and SN_{extrB} and region III prevails. Then, all extractive composition profiles reach the unstable node SN_{extrA} (Figure 11b $F_E/V = 0.5$). This shows the significance of the univolatility line in the synthesis of the homogeneous extractive distillation process because it sets limiting values of (F_E/V) . Here, $\alpha_{AB} = 1$ sets a maximum value $(F_E/V)_{max,B,R\infty}$ to recover (B). It can also be considered as a minimum value to recover (A) for any still composition. Below $(F_E/V)_{max,B,R\infty}$, (A) or (B) can be recovered in their respective feasible regions defined by the unstable extractive separatrix $UN_{extr} - S_{extr} - x_{AB}$. Above $(F_E/V)_{max,B,R\infty}$, only (A) is recovered whatever the composition. Compared to the conventional azeotropic distillation process where the feasible region is bounded by the distillation boundary, extractive distillation at infinite reflux makes the entire ternary diagram feasible to recover (A) when $(F_E/V) > (F_E/V)_{max,B,R\infty}$ and it is advantageous for the so called cyclic operation where the column operates under infinite reflux with accumulation of the distillate in the top tank.⁴⁸

As the entrainer is fed at infinite reflux, the still composition x_S moves towards (E) (Figure 10b). A peculiar behavior arises: when x_S is located in region I or II, component B is first settled at the column top but x_S may soon cross the extractive unstable separatrix into region III or IV due to the continuous feeding of E. Then, (A) replaces (B) at the column top. The temperature profile at the column top shows then a non conventional behavior as it suddenly decrease from $T_{boiling,B}$ to $T_{boiling,A}$. Further entrainer feeding keeps x_S in region III or IV. Considering operation under finite reflux ratio, unfeasible regions do not disappear even for high F_E/V reducing the recovery of (A).^{12,31,32} Furthermore, the still path can again wave along the extractive unstable separatrix and consequently the distillate temperature oscillates between $T_{boiling,B}$ and $T_{boiling,A}$.

Under finite reflux ratio, extractive profiles depend on the distillate composition (equation 2). Therefore, rectifying and extractive composition profiles maps must be computed for both possible distillate x_{DA} (Figure 12) and x_{DB} (Figure 13) for different F_E/V and R conditions.

For Figure 12a ($F_E/V = 0.5$ and $R = 10$), the shaded feasible region to recover x_{DA} does not span the entire composition diagram as in Figure 11b because an unstable extractive separatrix splits the triangle in two regions corresponding to regions I and III of Figure 10b. The ternary saddle S_{extr} and the stable node SN_{extrB} are located outside the composition triangle. UN_{extr} moves along with the extractive unstable separatrix towards the distillate x_{DA} . The rectifying separatrix also moves away from the binary side (B-E) and intersects the extractive separatrix in Figure 12a conditions. For Figure 12a, the shaded feasible region is the composition space on the right of the unstable extractive separatrix as all extractive profiles can intersect a rectifying profile reaching distillate x_{DA} . Recovery of (A) is not complete because the feasible region does not include the binary side (B-E). Lang et al. suggested to select R in order to provide a greater feasible region for distillate x_{DA} by extractive distillation than by azeotropic distillation.^{31,32} That reflux enables to set the extractive separatrix on the left of the rectifying separatrix. They found that an optimal reflux ratio exists for a given F_E/V .

The still path is determined by the cone of motion resulting from the addition of entrainer **E** along with the removal of distillate **D_A** (Figure 12a). After some operation time during extractive step 3, the still path may cross the stable rectifying separatrix and come into the unfeasible region I, so that distillate x_{DA} is no longer obtained. It is polluted by component (B) in an amount that will depend on the number of stages in each column section.

Increasing F_E/V moves SN_{extrA} closer to (E) or even outside the triangle (Figure 12b). The feasible region is then governed by the rectifying separatrix that is not influenced by F_E/V . Interception between extractive and rectifying profiles only occurs inside the feasible rectifying region (shady region in Figure 12b). A maximum value for F_E/V exists in this case for each reflux ratio if the number of stages in the extractive section is too high as was indicated by Lang et al.³¹

Figure 13a shows the extractive and rectifying profiles considering that chloroform (B) is distilled with purity x_{DB} under the same operating conditions of Figure 12a. Unlike to the previous case, there is no unstable extractive separatrix and only the stable rectifying separatrix determines the feasibility of separating (B). At $F_E/V = 0.5$ and $R = 10$, the stable rectifying separatrix is closer to the binary side (B-E) reducing the dimension of the feasible composition region for separating (B) even for batch azeotropic distillation process. In the upper feasible region all rectifying profiles end at the unstable node (B) whereas in the region below the rectifying separatrix, they end at the binary side (A-E). Regarding the extractive

profiles map and comparing to Figure 10b, S_{extr} lies out of the composition triangle and region III predominates, where all extractive profiles reach the binary side (A-E). Therefore component (B) can be distilled only if two conditions are fulfilled: first extractive and rectifying profiles intercept into the shaded region above the stable rectifying separatrix (Figure 13a); second the number of theoretical stages in the extractive section is lower than a given $N_{B,MAX}$ value to prevent extractive profile from crossing the stable rectifying separatrix and from intercepting rectifying profiles that reach the (A-E) edge.

Similar to Figure 10b, as F_E/V decreases, the stable extractive separatrix and SN_{extrB} appear (Figure 13b for $F_E/V=0.05$ and $R=10$). But, unlike to the total reflux operation (Figure 10b), the saddle point S_{extr} is located above the univolatility line and also SN_{extrA} lies outside the composition space. Due to the proximity of rectifying and extractive separatrices, interception between rectifying and extractive profile occurs mainly in the corresponding feasible region for each component (A) and (B). Hence, the maximum number of stages for extractive section is not as critical as in Figure 13a, except in the small region between both separatrices.

In this region, normally belonging to the feasible region to distillate (B) as extractive profiles can intercept a rectifying profile connected to the unstable (B), a number of the equilibrium stage of the extractive section larger than a limit value ($N_{B,MAX}$) will lead to recover a binary mixture (A-E) instead of (B) because, extractive profiles can then cross the stable rectifying separatrix and intercept any rectifying profile located in the region below and going to the (A-E) edge.

In summary for class 1.0-2 separation, good recovery of (A) or (B) is incomplete at finite reflux because of the existence of the stable rectifying separatrix even if the unstable extractive separatrix doesn't exist. The recovery of distillate x_{DB} is more restricted than distillate x_{DA} because the unstable node (B) is located on the convex side of the curved rectifying separatrix, in the C-shape elementary cell I region. As Kiva et al. pointed out, the residue curve shape is determined by the presence of the unidistribution line and of the univolatility line.⁷ For class 1.0-2, unidistribution line $K_B = 1$ exists (Figure 2) and the residue curve going from (A) to (E) shows a maximum value crossing the unidistribution line, resulting in a significant curvature of the rectifying stable separatrix locating the rcm unstable node (A) on the concave side. Conversely, the unidistribution line $K_A = 1$ also exists but S-shape residue curves coming from (B) present also an inflexion point where they cross the $\alpha_{AB} = 1$ curve reaching the binary side (B-E). Hence (B) lies on the convex side of the rectifying stable separatrix because no additional unidistribution line exists between $\alpha_{AB} = 1$

and the rcm stable node (E).⁷ So, class 1.0-2 diagram exhibits a curved stable separatrix making easier to recover the more volatile (A) than (B) by using azeotropic or extractive distillation process.

6.2.2 Class 1.0-2 case b: $\alpha_{AB} = 1$. Curve reaching the binary side (A-E). Separation of chloroform – vinyl acetate with heavy butyl acetate illustrates the case when the univolatility line α_{AB} reaches the binary side (A-E) (Figure 9b case). Rcm stability is the same as in Figure 9a (see Figure 14a). The unique univolatility curve, $\alpha_{AB} = 1$ starts at the maximum boiling azeotrope $T_{\max} \text{ azeo}_{AB}$ and reaches the binary side (A-E). As both chloroform (A) and vinyl acetate (B) are the most volatile in the region where there exists a residue curve with decreasing temperature from (E) to their location, both (A) or (B) are possible distillate of extractive distillation process. They can also be obtained by azeotropic distillation as they are rcm unstable nodes in their respective distillation region. The rectifying stable separatrix is slightly curved in the region containing (B) for the same reasons that applied to (A) for the previous class 1.0-2 case *a*. Nevertheless, unlike the acetone – chloroform – benzene mixture, the rectifying stable separatrix curvature is small and does not provide a good enough recovery of component (B) by azeotropic distillation, leading more opportunity of applying the extractive distillation process.

Figure 14b displays the rectifying profiles going through $x_{DA} = \{0.990, 0.005, 0.005\}$ and $x_{DB} = \{0.005, 0.990, 0.005\}$ and the extractive composition profiles for $F_E/V = 0.5$, computed at infinite reflux. Figure 14b displays the extractive map features similar as in Figure 10b with four regions due to the extractive separatrices crossing at the saddle S_{extr} that moves along the univolatility line under infinite reflux ratio conditions. The unstable extractive separatrix between UN_{extr} at vertex (E) and x_{AB} located on the binary side chloroform – vinyl acetate at approximately 45% of chloroform defines two feasible areas.

For a still composition in the region above the unstable extractive separatrix $UN_{extr} - S_{extr} - x_{AB}$ (regions I and II), distillate x_{DB} can be settled into the condenser; below (regions III and IV), distillate x_{DA} does, under infinite reflux operation. Similarly to the previous case, continuous feeding of butyl acetate enlarges the feasible region for distillate x_{DB} because the unstable extractive separatrix is farther from the binary side (B-E) than the rectifying stable separatrix (Figure 14b). In regions I and II, all composition profiles reach the stable node SN_{extrB} and no minimum value of the entrainer flowrate $(F_E/V)_{\min B}$ exists to recover distillate x_{DB} . In regions III and IV, composition profiles reach the stable node SN_{extrA} and enable to recover distillate x_{DA} but, there is a maximum value of entrainer flowrate $(F_E/V)_{\max A, R\infty}$

because $\alpha_{AB} = 1$ curve reaches the binary side (A-E). At infinite reflux and $(F_E/V) < (F_E/V)_{maxA,R\infty}$, the still path x_S may also cross the extractive unstable separatrix for an initial composition located in region III or IV (Figure 14b) and component (B) will then pollute the distillate.

As F_E/V increases above $(F_E/V)_{maxA,R\infty}$, the saddle point S_{extr} merges with SN_{extrA} and all extractive liquid profiles reach the only stable node SN_{extrB} and the region I overcomes the ternary diagram similarly to Figure 11b so that x_{DB} is always distilled. As said before, this behavior would be interesting is the case of a cyclic operation extractive distillation process.

As the reflux ratio becomes finite, such features also hold at large F_E/V and large reflux ratio (Figure 15, $F_E/V = 1.5$ and $R = 30$) but exact rectifying and extractive regions must be computed for various finite R and F_E/V values for the recovery of either component (B) (x_{DB}) or (A) (x_{DA}). We present only the case for the recovery of distillate x_{DB} . BatchColumn® simulation results are displayed for a distillation column having 50 theoretical stages with butyl acetate fed at tray 5 from the top. The vapour overflow from the boiler and the entrainer flowrate were defined to provide a ratio of $F/V = 1.5$ approximately inside the extractive column section. Trays and condenser liquid holdup were set small.

In Figure 15, the initial still composition x_{S0} lies in the rcm distillation region where chloroform (A) is the unstable node. So, after step (1) of batch extractive distillation process (infinite reflux, without entrainer feeding) (A) is obtained overhead. During step (2), the butyl acetate is fed and vinyl acetate (B) quickly replaces (A) at the column top as extractive profile from x_{S1} intersects a rectifying profile going to x_{DB} . When the distillate removal starts (step 3, $F_E/V = 1.5$ and $R = 30$), the vector cone direction of the still path is set by the removal of x_{DB} and the continuous entrainer feeding of pure butyl acetate x_E (Figure 15). Process is feasible as the rectifying and extractive profiles intersect (shown for x_{S3} composition). Note that the interception occurs close to the stable node SN_{extrB} estimated by the simplified model.

However, an unfeasible region for recovering distillate x_{DB} exists below the extractive unstable separatrix. After some operation time, the still path moves below the extractive unstable separatrix and distillate is polluted first by chloroform and later by butyl acetate as shown by the distillate path in Figure 15. Simulation finished when the still contained less than 1% of vinyl acetate (x'_{S3}) but pollution of the distillate led to an average distillate purity below the expected 99% of vinyl acetate. To get $x_{DB,vinyl\ acetate} = 0.99$, a higher reflux ratio should be defined before the still path crosses the extractive unstable separatrix, for example $R = 60$.

Overall, the feasible region for extractive distillation remains much larger than the feasible region for azeotropic distillation bounded by the rectifying stable separatrix until $R \cong 4$ (Figure 16a). Depending on the initial still composition, an optimal reflux policy can be established in order to reduce the total entrainer consumption and the operation time.

Influence of F_E/V on the feasibility region shows that a low value is preferable. For $F_E/V = 5$ at $R = 30$ (Figure 16b), the extractive unstable separatrix has disappeared and the feasibility region for vinyl acetate is now imposed by the rectifying stable separatrix because the interception between the extractive and rectifying liquid profile is only possible in the shaded region. This behaviour establishes a maximum value for F/V when the process is performed at finite reflux ratio.

Similar to the separation of acetone – chloroform using benzene, high recovery and purity of vinyl acetate requires an increasing reflux ratio policy while the still is depleted of component (B). But, in this case, extractive distillation is compulsory because the small curvature of the stable separatrix prevents to run azeotropic distillation with a good performance.

7. Conclusions

Feasibility of homogeneous batch extractive distillation for the separation of an A-B mixture feeding entrainer E is ensured when the still composition is linked to the expected distillate by intersecting extractive and rectifying composition profiles. It was formerly assessed by computing systematically rectifying and extractive composition profile maps under many reflux ratio and entrainer flowrate conditions. In the present work, we have evidenced the importance of the univolatility curve $\alpha_{AB} = 1$ and of the location of its interception with the composition triangle A-B-E not only for the separation of a minimum boiling azeotrope with a heavy entrainer (class 1.0-1a) but for all cases.

The results displayed in this manuscript are an exhaustive complement of former methods proposed by Laroche et al.¹⁴ and Pöllmann and Blass²³ with the light on ternary diagram properties brought by Hilmen et al.⁸ and Kiva et al.⁷ that is synthesized in the enunciation of a general criterion, stating that: “*homogeneous batch extractive distillation of a (A) – (B) mixture with entrainer (E) feeding is feasible if there exists a residue curve connecting (E) to (A) or (B) following a decreasing (a) or increasing (b) temperature direction inside the region where (A) or (B) is the most volatile (a) or the heaviest (b) component of the mixture.*”.

Then thermodynamic topological features concerning the 9 cases published in the literature when (E) forms no new azeotrope with either (A) or (B) have been reviewed (ternary diagram classes 0.0-1, 1.0-1a, 1.0-2 and 1.0-1b), especially the occurrence of $\alpha_{AB} = 1$ curves. Detailed illustration of the splitting of minimum or maximum boiling azeotropes with a heavy entrainer was presented; class 1.0-1a (figure 4) or 1.0-2 respectively (figure 9). For both classes, two alternative intersections of the $\alpha_{AB} = 1$ with the triangle edge exist, some not previously studied. Operation under infinite reflux was governed by the general feasibility criterion and existence or not of a limit value of the entrainer flowrate could be guessed by using thermodynamic insight without any composition profile calculation. The extractive singular point located at the azeo_{AB} for infinitesimally small entrainer flowrate always moves on the univolatility line at infinite reflux operation. Operation under finite reflux additionally depends on the occurrence of an extractive unstable separatrix which behavior can be simply predicted from thermodynamic insight related to the stability of the extractive composition profile map singular points.

For class 1.0-1a (T_{\min} azeo_{AB} with heavy entrainer), the general feasibility criterion shows that under infinite reflux condition, either (A) or (B) can be distilled depending whether $\alpha_{AB} = 1$ intersects the (A-E) or the (B-E) edge, with a minimum entrainer flowrate required. At finite reflux, an unfeasible region occurs because of the extractive unstable separatrix. Operation should start at low reflux ratio and then at a higher reflux ratio to prevent the still path to move into the unfeasible region.

For class 1.0-2 (T_{\min} azeo_{AB} with heavy entrainer), the general feasibility criterion shows that both (A) and (B) can be distilled by batch extractive distillation. But the process has its best potential for the component that is located in the concave side of the rcm stable separatrix where rcm have a C-shape. Even at infinite reflux ratio, an unfeasible region occurs (either for (A) or (B)) because of the extractive unstable separatrix. Depending whether $\alpha_{AB} = 1$ intersects the (A-E) or the (B-E) edge, a maximum entrainer flowrate exists for (A) or (B) respectively, also setting a limit above which (B) or (A) alone is recovered whatever the still composition. Under finite reflux ratio conditions, the unfeasible region expands as the reflux ratio decreases. That imposes an operation at large reflux ratio which is not so economically viable. Nevertheless, the extractive process remains a viable alternative to azeotropic distillation, that is always possible for class 1.0-2 (both (A) and (B) are rcm unstable node), because the extractive feasible region can be made significantly larger than the azeotropic feasible region. It is also shown that the still path can cross into the unfeasible region, leading

to an unconventional temperature vs time behavior: temperature could decrease as time increases.

Part II presents cases related to the separation of low relative volatility mixtures (0.0-1 class) using heavy homogeneous entrainer.

Literature Cited

- (1) Widagdo S.; Seider W.D. Azeotropic Distillation. *AIChE J.* **1996**, *42*, 96-126.
- (2) Seider, J.D.; Sirola, J.J.; Barnicki, S.D. *Perry's Chemical Engineers' Handbook. Distillation*. Section 13, pp. 13-79. 7th Edition. McGraw-Hill, New York. **1997**.
- (3) Stichlmair, J.; Fair, J. D. *Distillation – Principles & Practice*. John Wiley, London. **1998**.
- (4) Doherty M.F.; Malone M.F. *Conceptual Design of Distillation Systems*. Mc Graw-Hill, New York. **2001**.
- (5) Van Dongen, D.B.; Doherty, M.F. Design and Synthesis of Homogeneous Azeotropic Distillation. 1. Problem Formulation for a Single Column. *Ind. Eng. Chem. Fundam.* **1985**, *24*, 454-463.
- (6) Lelkes, Z.; Lang, P.; Benadda, B.; Moszkowicz, P. Feasibility of Extractive Distillation in a Batch Rectifier. *AIChE J.* **1998**, *44*, 810-822.
- (7) Kiva, V.N.; Hilmen, E.K.; Skogestad, S. Azeotropic Phase Equilibrium Diagrams: A Survey. *Chem. Eng. Sci.* **2003**, *58*, 1903-1953.
- (8) Hilmen, E. K.; Kiva, V. N.; Skogestad, S. Topology of Ternary VLE Diagrams: Elementary Cells. *AIChE J.* **2002**, *48*(4), 752-759.
- (9) Rodríguez-Donis, I.; Gerbaud, V.; Joulia, X. Entrainer Selection Rules for the Separation of Azeotropic and Close Boiling Point Mixtures by Homogeneous Batch Distillation. *Ind. Chem. Eng. Res.* **2001**, *40*(12), 2729-2741.
- (10) Rodríguez-Donis, I.; Gerbaud, V.; Joulia, X. Heterogeneous Entrainer Selection Rules for the Separation of Azeotropic and Close Boiling Point Mixtures by Heterogeneous Batch Distillation. *Ind. Chem. Eng. Res.* **2001**, *40*(22), 4935-4950.
- (11) Skouras, S.; Kiva, V.; Skogestad S. Feasible Separations And Entrainer Selection Rules for Heteroazeotropic Batch Distillation. *Chem. Eng. Sci.* **2005**, *60*(11), 2895-2909.
- (12) Steger, C.; Varga, V.; Horvath, L.; Rev, E.; Fonyo, Z.; Meyer, M.; Lelkes, Z. Feasibility of Extractive Distillation Process Variants in Batch Rectifier Column. *Chem. Eng. Process.* **2005**, *44*, 1237-1256.
- (13) Varga, V. Distillation Extractive Discontinue dans une Colonne de Rectification et dans une Colonne Inverse. *Ph.D. Thesis*, Toulouse. **2006**.
- (14) Laroche, L.; Bekiaris, N.; Andersen, H.W.; Morari, M. Homogeneous Azeotropic Distillation: Comparing Entrainers. *The Can. J. Chem. Eng.* **1991**, *69*, 1302-1319.
- (15) Knapp, J. P.; Doherty, M. F. Minimum Entrainer Flow for Extractive Distillation: A Bifurcation Theoretic Approach. *AIChE J.* **1994**, *40*(2), 243-268.

- (16) Laroche, L.; Bekiaris, N.; Andersen, H.W.; Morari M. The Curious Behavior of Homogeneous Azeotropic Distillation – Implications for Entrainer Selection. *AIChE J.* **1992**, *38*, 1309-1328.
- (17) Hilmen, E. K. Separation of Azeotropic Mixtures: Tools for Analysis and Studies on Batch Distillation Operation. *Ph.D. Thesis*. Norwegian University of Science and Technology, Trondheim, Norway, **2000**.
- (18) Brüggemann, S.; Marquardt, W. Shortcut Methods for Nonideal Multicomponent Distillation: 3. Extractive Distillation Columns. *AIChE J.* **2004**, *50*, 1129-1149.
- (19) Gerbaud, V.; Joulia, X.; Rodriguez-Donis, I.; Baudouin, O.; Rosemain, O.; Vacher, A.; Castelain, P. Practical Residue Curve Map Analysis Applied to Solvent Recovery in Non-Ideal Binary Mixtures by Batch Distillation Processes. *Chem. Eng. Process.* **2006**, *45*(8), 672-683.
- (20) Kossack, S.; Kraemer, K.; Gani, R.; Marquardt, W. A Systematic Synthesis Framework for Extractive Distillation Processes. *Proceedings of European Congress of Chemical Engineering (ECCE-6)*. Copenhagen, 16-20 September, **2007**.
- (21) Prausnitz, J.M.; R.N. Lichtenhaler; Azevedo, E.G. *Molecular thermodynamics of fluid-phase equilibria*. Prentice – Hall, Engelwood Cliffs. New York, **1986**.
- (22) Fredenslund, A.; R.L. Jones; J.M. Prausnitz, Group-Contribution Estimation of Activity Coefficients in Non-Ideal Liquid Mixtures. *AIChE J.* **1975**, *21*, 1086 – 1099.
- (23) Pöllmann, P.; Blass, E. Best Products of Homogeneous Azeotropic Distillations. *Gas Sep. and Purif.* **1994**, *8*, 194-228.
- (24) Yatim H.; Moszkowicz, P.; Otterbein M.; Lang, P. Dynamic Simulation of a Batch Extractive Distillation Process. *Comput. Chem. Eng.* **1993**, *17*, S57-S62.
- (25) Lang, P.; Yatim, H.; Moszkowicz, P.; Otterbein, M. Batch Extractive Distillation under Constant Reflux Ratio. *Comput. Chem. Eng.* **1994**, *18*, 1057-1069.
- (26) Hunek, J.; Gal, S.; Posel, F.; Glavic, P. Separation of an Azeotropic Mixture by Reverse Extractive Distillation. *AIChE J.* **1989**, *35*(7), 1207-1210.
- (27) Bernot, C.; Doherty, M.; Malone M.F. Patterns of Composition Change in Multicomponent Batch Distillation. *Chem. Eng. Sci.* **1990** *45*, 1207-1221.
- (28) Milani, S.M. Optimisation of Solvent Feed Rate for Maximum Recovery of High Purity Top Product in Batch Extractive Distillation. *Chem. Eng. Res. Des.* **1999**, *77*, 469-470.
- (29) Lang, P.; Lelkes, Z.; Moszkowicz P.; Otterbein M.; Yatim H. Different Operational Policies for the Batch Extractive Distillation. *Comp. Chem. Eng.* **1995**, *19*, S645-S650.
- (30) Lang, P.; Lelkes, Z.; Otterbein M.; Benadda, B.; Modla, G. Feasibility Studies for Batch Extractive Distillation with a Light Entrainer. *Comput. Chem. Eng.* **1999**, *23*, S93-S96.
- (31) Lang, P.; Modla, G.; Benadda, B.; Lelkes, Z. Homoazeotropic Distillation of Maximum Azeotropes in a Batch Rectifying Column with Continuous Entrainer Feeding. I. Feasibility Studies. *Comput. Chem. Eng.* **2000**, *24*, 1665-1671.
- (32) Lang, P.; Modla, G.; Kotai, B.; Lelkes, Z.; Moszkowicz, P. Homoazeotropic Distillation of Maximum Azeotropes in a Batch Rectifying Column with Continuous Entrainer Feeding II. Rigorous Simulation Results. *Comput. Chem. Eng.* **2000**, *24*, 1429-1435.

- (33) Lelkes, Z.; Lang, P.; Moszkowicz, P.; Benadda, B.; Otterbein M. Batch Extractive Distillation: The Process and the Operational Policies. *Chem. Eng. Sci.* **1998**, *53*(7), 1331-1348.
- (34) Lelkes, Z.; Lang, P.; Otterbein, M. Feasibility and Sequencing Studies for Homoazeotropic Distillation in a Batch Rectifying Column with Continuous Entrainer Feeding. *Comp. Chem. Eng.* **1998**, *22*, S653-S656.
- (35) Lelkes, Z.; Rev, E.; Steger, C.; Fonyo, Z. Batch extractive distillation of maximal azeotrope with middle boiling entrainer. *AIChE J.* **2002**, *48*(11), 2524-2536.
- (36) Lelkes, Z.; Rev, E.; Steger, C.; Varga, V.; Fonyo, Z.; Horvath, L. Batch Extractive Distillation with Intermediate Boiling Entrainer. *Proceedings ESCAPE-13*. (Eds. Kraslawski, A. and Turunen, I.) 197-202, **2003**.
- (37) Rev, E.; Lelkes, Z.; Varga, V.; Steger, C.; Fonyo, Z. Separation of a Minimum-Boiling Azeotrope in a Batch Extractive Rectifier with an Intermediate-Boiling Entrainer. *Ind. Eng. Chem. Res.* **2003**, *42*(1), 162-174.
- (38) Varga, V.; Rev, E.; Gerbaud, V.; Lelkes, Z.; Fonyo, Z.; Joulia, X. Batch Extractive Distillation with Light Entrainer. *Chem. Biochem. Eng. Q.* **2006**, *20*(1), 1-24.
- (39) Gmehling, J.; Menke, J.; Krafczyk J.; Fischer, K. *Azeotropic Data*, 2nd ed. Wiley-VCH Editor, **1994**.
- (40) Bernot C.; Doherty M.F.; Malone M.F. Feasibility and Separation Sequencing in Multicomponent Batch Distillation. *Chem. Eng. Sci.* **1991**, *46*, 1311-1326.
- (41) Reshetov, S.A.; Kravchenko S.V. Statistics of Liquid-Vapor Phase Equilibrium Diagrams for Various Ternary Zeotropic Mixtures. *Theor. Found. Chem. Eng.* **2007**, *41*(4), 451-453.
- (42) Rodríguez-Donis, I.; Gerbaud, V.; Joulia, X. New Thermodynamic Insights on the Feasibility of Homogeneous Batch Extractive Distillation. II. Separation of Low Relative Volatility Binary Mixtures. Submitted to *Ind. Chem. Eng. Res.* **2008**.
- (43) Frits, E.R.; Lelkes, Z.; Fonyo, Z.; Rev, E.; Markot, M.Cs. Finding Limiting Flows of Batch Extractive Distillation with Interval Arithmetics. *AIChE J.* **2006**, *52*(9), 3100-3108.
- (44) ProSim S.A. <http://www.prosim.net>
- (45) Van Dongen D.B.; Doherty M.F. On the Dynamics of Distillation Process - VI. Batch Distillation. *Chem. Eng. Sci.* **1985**, *40*, 2087-2093.
- (46) Bernot C.; Doherty M.F.; Malone M.F. Feasibility and Separation Sequencing in Multicomponent Batch Distillation. *Chem. Eng. Sci.* **1991**, *46*, 1311-1326.
- (47) Dussel R.; Stichlmair J. Separation of Azeotropic Mixtures by Batch Distillation Using an Entrainer. *Comput. Chem. Eng.* **1995**, *19*, S113-S118.
- (48) Sorensen, E. A Cyclic Operation Policy for Batch Distillation. Theory and Practice. *Comp. & Chem. Eng.* **1999**, *23*, 533-542

FIGURE CAPTION

Figure 1. Ternary VLE diagrams for the separation of non ideal mixtures by homogeneous extractive distillation using light, intermediate or heavy entrainers forming no new azeotrope. (statistics from Hilmen et al.⁸)

Figure 2. Unidistribution and univolatility lines for the four ternary diagram involved in homogeneous extractive distillation process.

Figure 3. Reflux and entrainer feed flowrate influence on class 1.0-1a diagrams for the batch homogeneous extractive rectification of a minimum boiling azeotrope with a heavy entrainer.

Figure 4. Ternary diagram for minimum boiling azeotrope separation using heavy entrainers.

Figure 5. Acetone – heptane – toluene thermodynamic properties and extractive composition profiles. (a) $F_E/V \leq (F_E/V)_{min}$. (b) Extractive composition profile map for $F_E/V > (F_E/V)_{min}$.

Figure 6. Extractive composition profile map and feasible regions for $F/V = 0.2$ and $R = 5$.

Figure 7. Acetone – methanol - chlorobenzene thermodynamic properties and extractive composition profiles. (a) $F_E/V \leq (F_E/V)_{min}$. (b) Extractive composition profile map for $F_E/V > (F_E/V)_{min}$.

Figure 8. Extractive composition profile map and rigorous simulation results for $F/V = 1$ and $R = 10$.

Figure 9. Ternary diagram for maximum boiling azeotrope separation using heavy entrainers.

Figure 10. Feasibility of the batch extractive distillation operating at infinite reflux ratio. (a) Thermodynamic features. (b) Extractive composition profile map at $(F_E/V) = 0.05$

Figure 11. Extractive liquid profile map for the ternary system acetone – chloroform - benzene at infinite reflux ratio. (a) $F_E/V = 0.2$ (b) $F_E/V = 0.5$

Figure 12. Extractive and rectifying profile map for operation at finite reflux ratio. Acetone (A) is drawn as distillate product.

Figure 13. Extractive and rectifying profile map for operation at finite reflux ratio. Chloroform (B) is drawn as distillate product.

Figure 14. Feasibility analysis of the separation of chloroform - vinyl acetate using butyl acetate at infinite reflux ratio. (a) Residue curve map. (b) Extractive composition profile map at $(F_E/V) = 0.5$

Figure 15. Extractive composition profile map and simulation results for $F_E/V = 1.5$ and $R = 30$

Figure 16. Influence of R and F_E/V on the feasible region to recover x_{DB} .

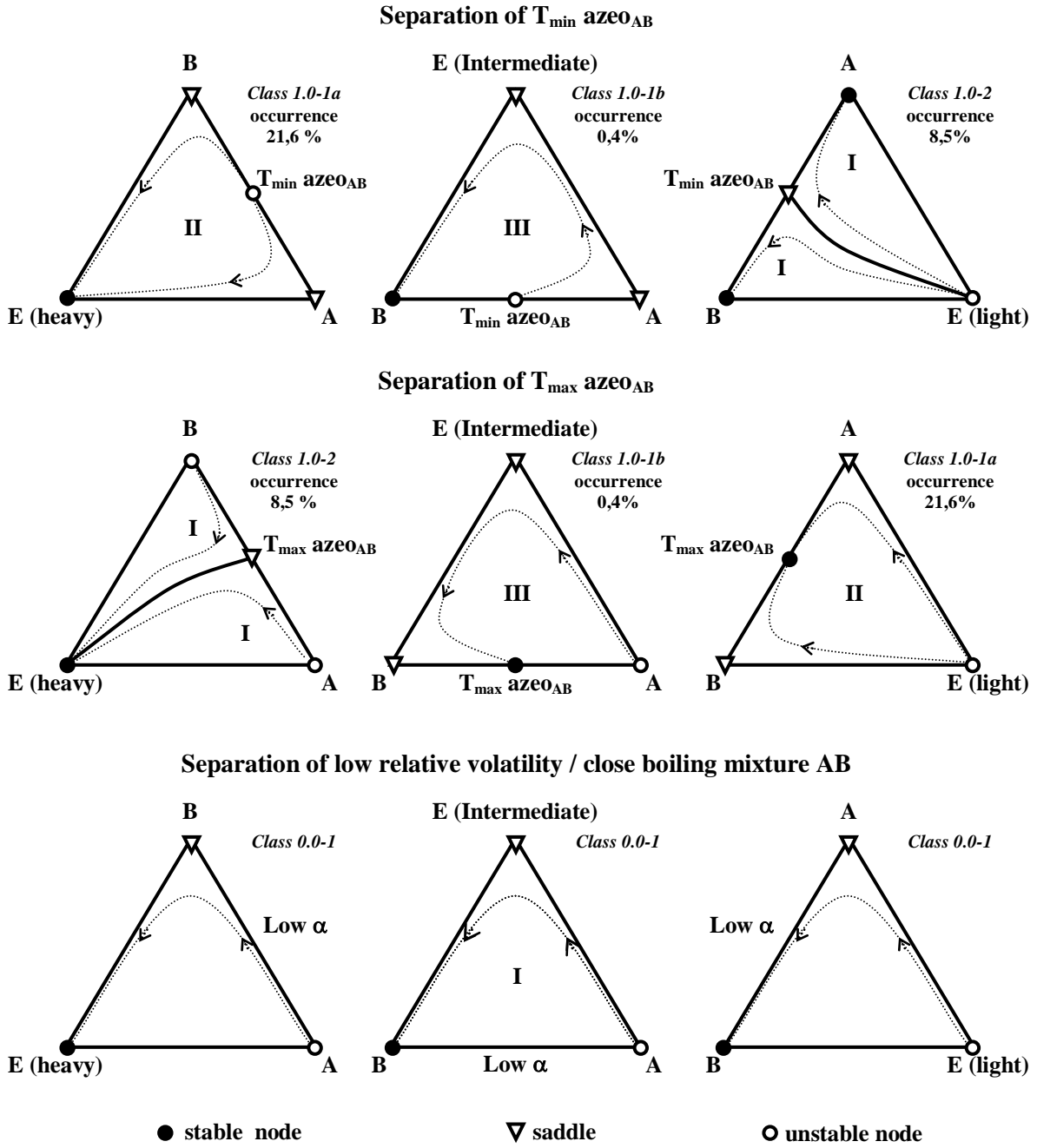


Figure 1. Ternary VLE diagrams for the separation of non ideal mixtures by homogeneous extractive distillation using light, intermediate or heavy entrainers forming no new azeotrope. (statistics from Hilmen et al.⁸)

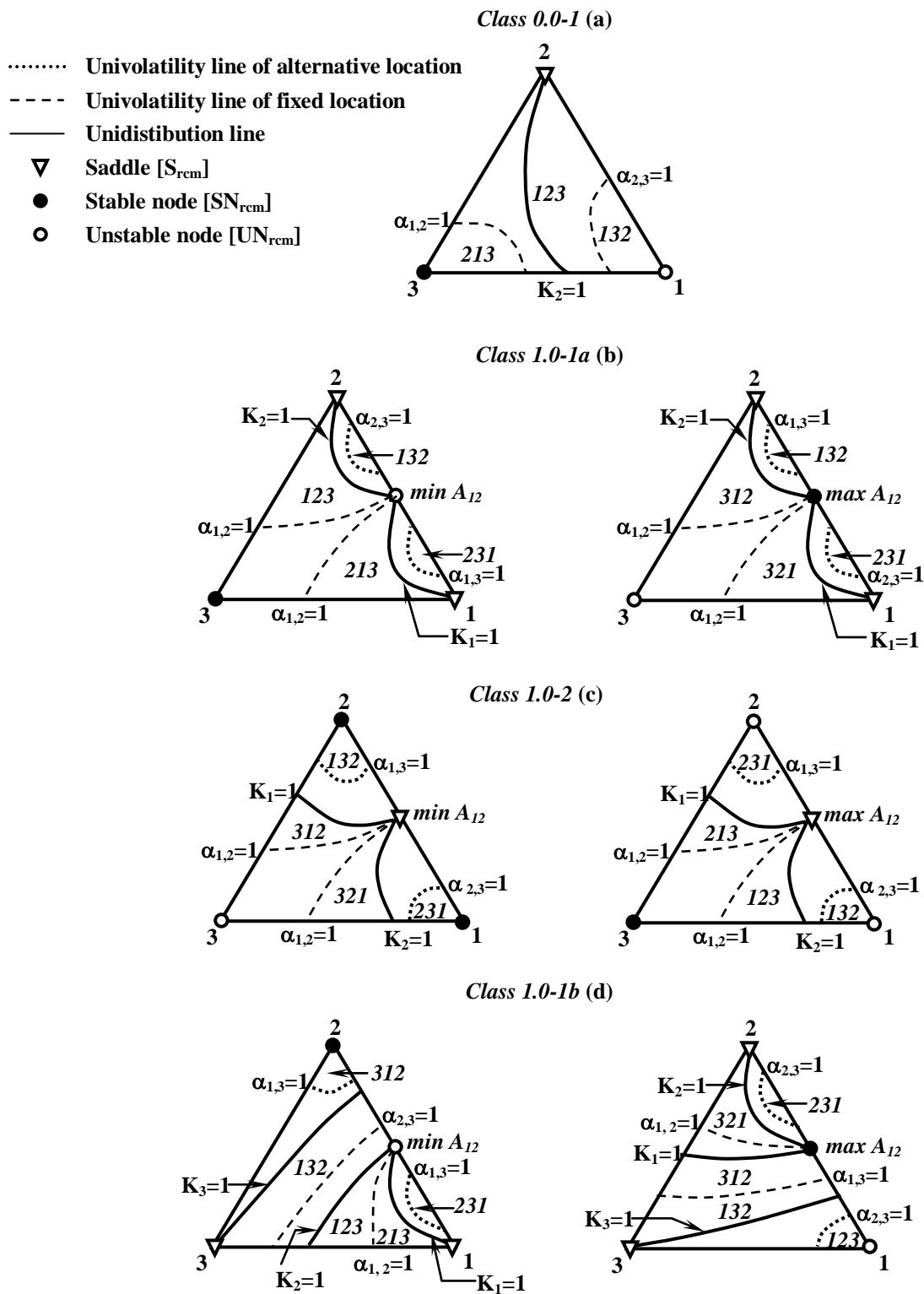


Figure 2. Unidistribution and univolatility lines for the four ternary diagram involved in homogeneous extractive distillation process.

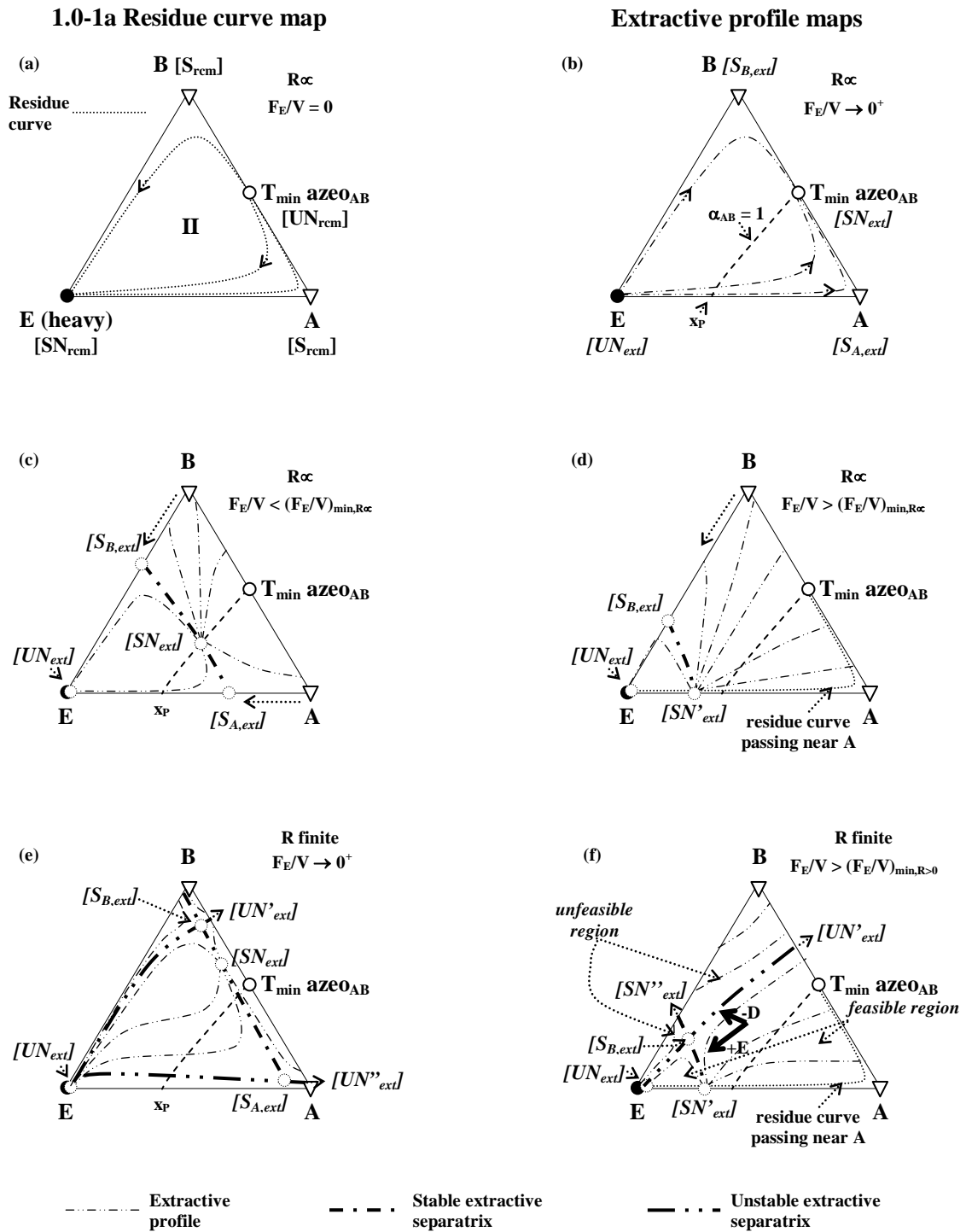


Figure 3. Reflux and entrainer feed flowrate influence on class 1.0-1a diagrams for the batch homogeneous extractive rectification of a minimum boiling azeotrope with a heavy entrainer.

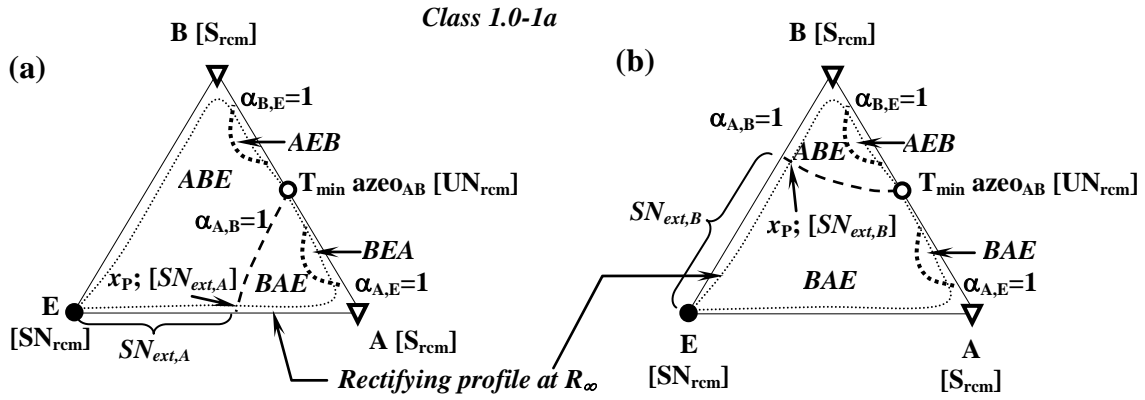


Figure 4. Ternary diagram for minimum boiling azeotrope separation using heavy entrainers.

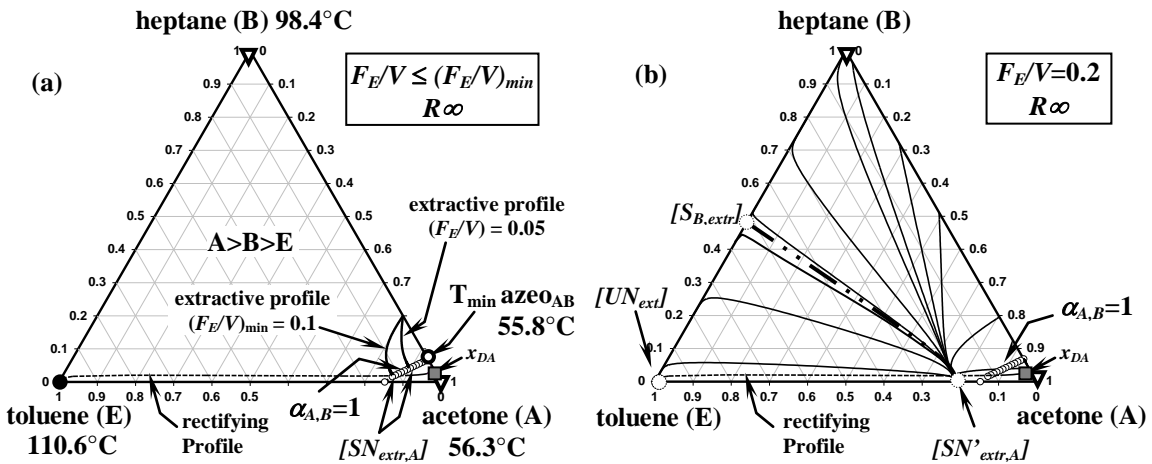


Figure 5. Acetone – heptane – toluene thermodynamic properties and extractive composition profiles. (a) $F_E/V \leq (F_E/V)_{min}$. (b) Extractive composition profile map for $F_E/V > (F_E/V)_{min}$.

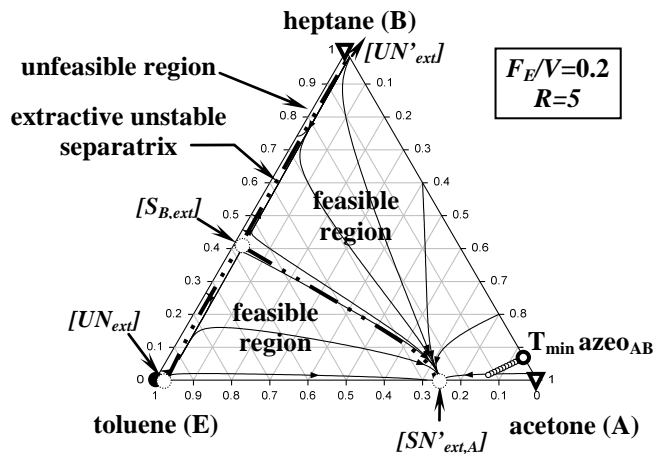


Figure 6. Extractive composition profile map and feasible regions for $F/V = 0.2$ and $R = 5$.

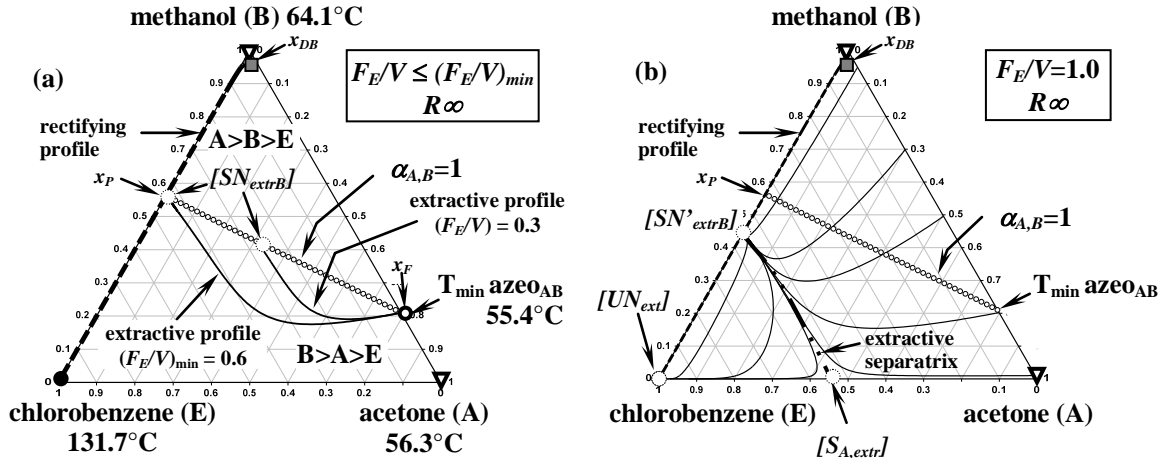


Figure 7. Acetone – methanol - chlorobenzene thermodynamic properties and extractive composition profiles. (a) $F_E/V \leq (F_E/V)_{min}$. (b) Extractive composition profile map for $F_E/V > (F_E/V)_{min}$.

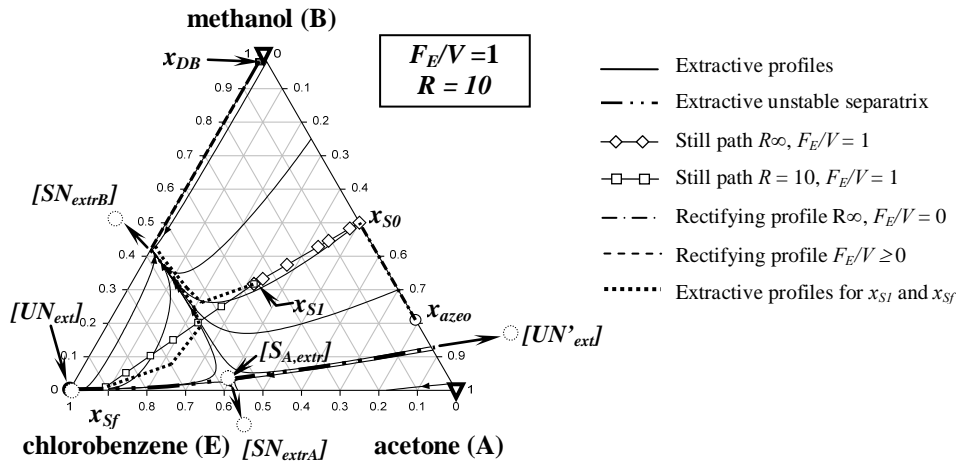


Figure 8. Extractive composition profile map and rigorous simulation results for $F/V = 1$ and $R = 10$.

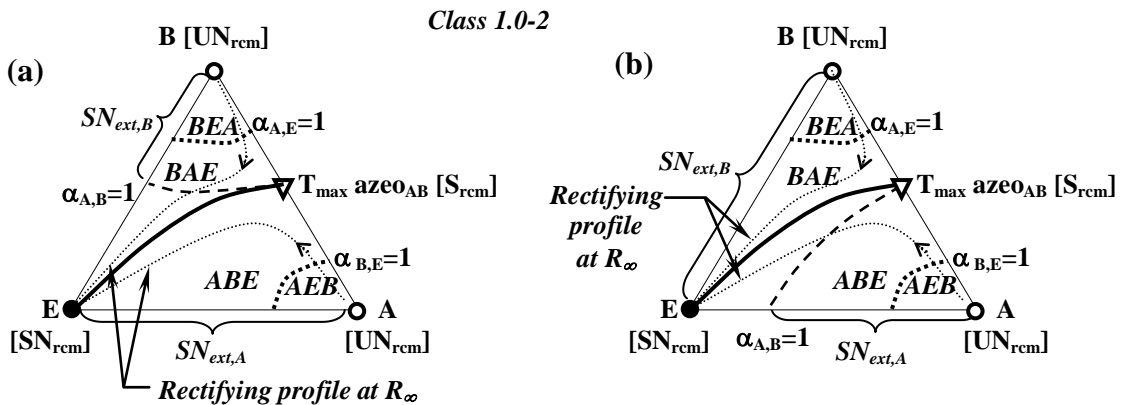


Figure 9. Ternary diagram for maximum boiling azeotrope separation using heavy entrainers.

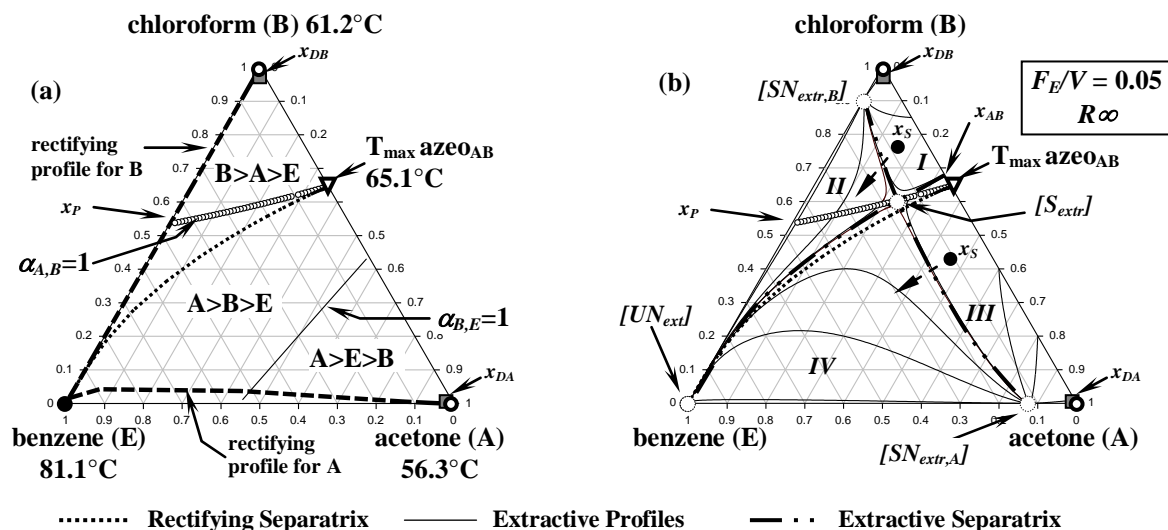


Figure 10. Feasibility of the batch extractive distillation operating at infinite reflux ratio. (a) Thermodynamic features. (b) Extractive composition profile map at $(F_E/V) = 0.05$

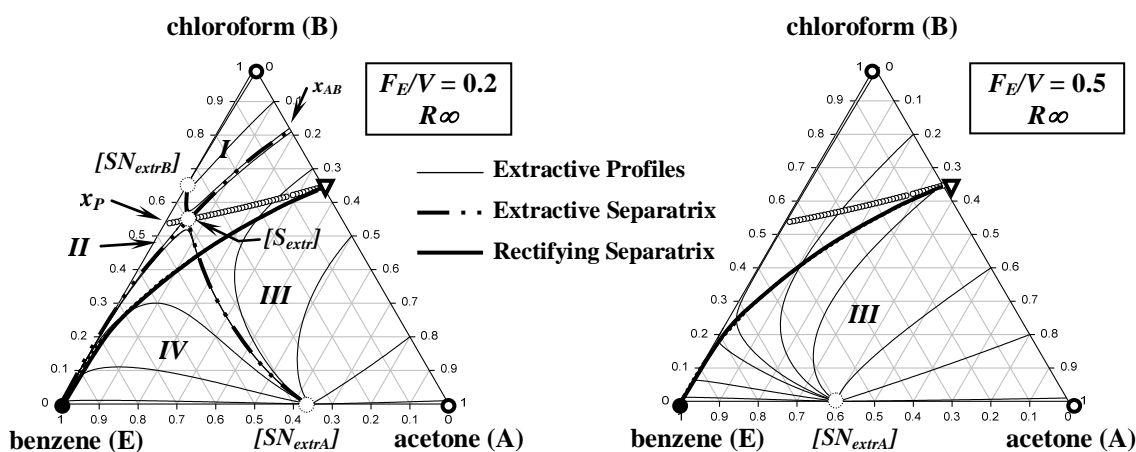


Figure 11. Extractive liquid profile map for the ternary system acetone – chloroform – benzene at infinite reflux ratio. (a) $F_E/V = 0.2$ (b) $F_E/V = 0.5$

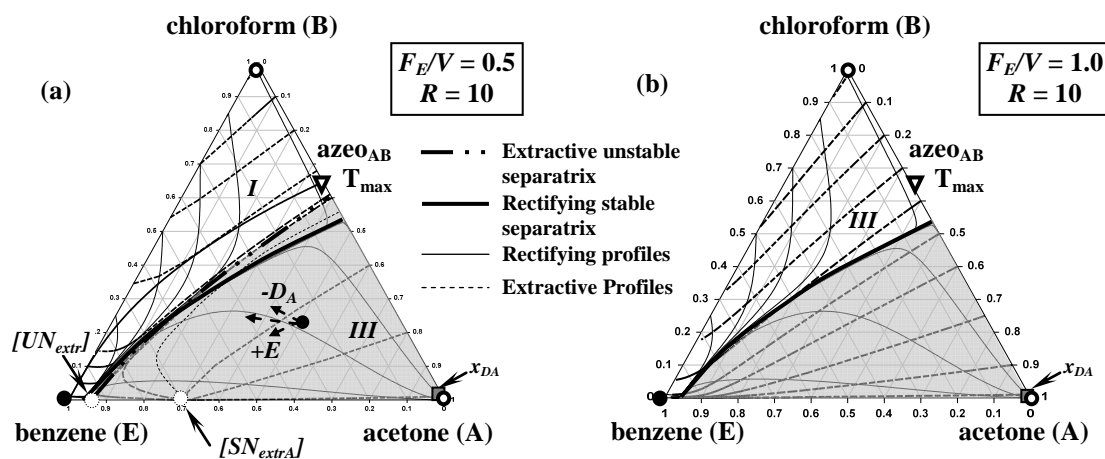


Figure 12. Extractive and rectifying profile map for operation at finite reflux ratio. Acetone (A) is drawn as distillate product.

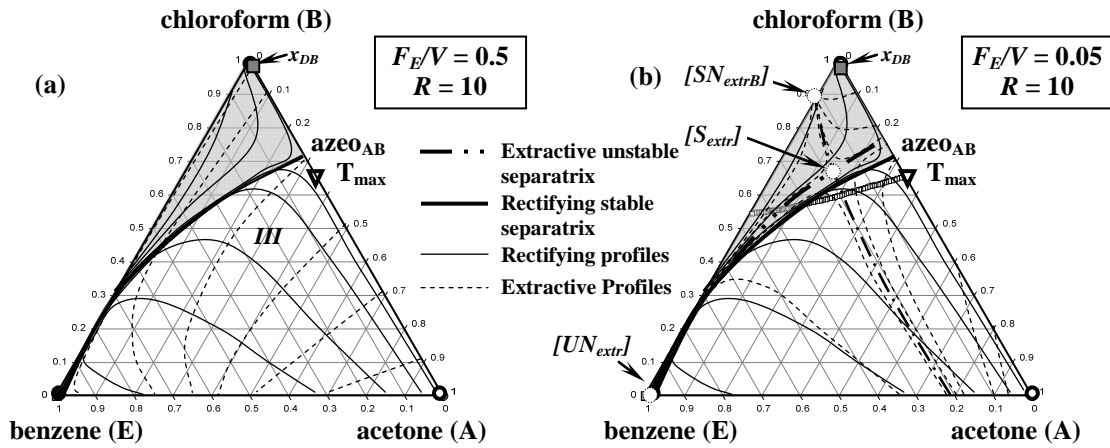


Figure 13. Extractive and rectifying profile map for operation at finite reflux ratio. Chloroform (B) is drawn as distillate product.

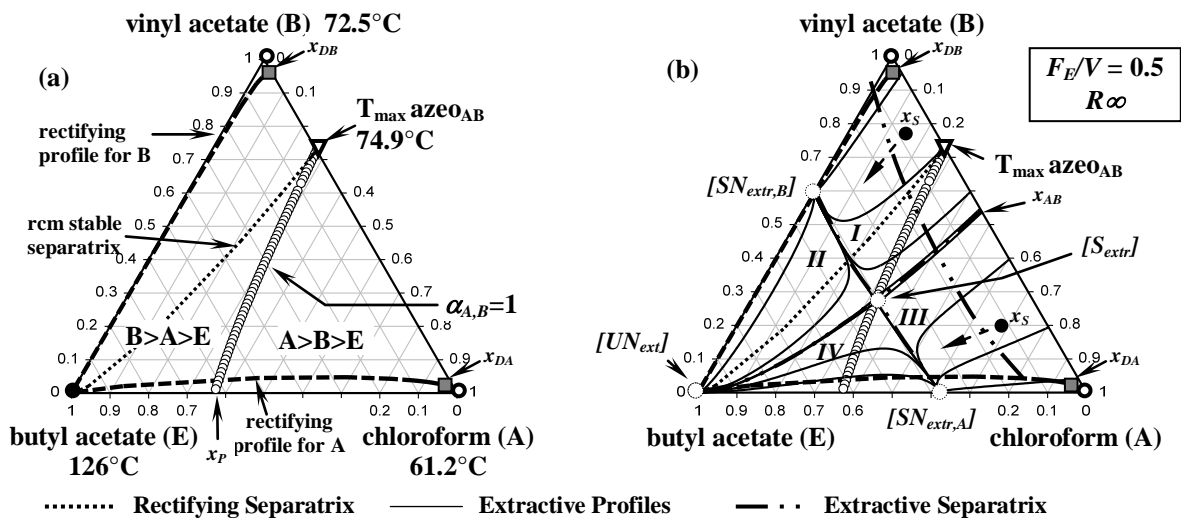


Figure 14. Feasibility analysis of the separation of chloroform - vinyl acetate using butyl acetate at infinite reflux ratio. (a) Residue curve map. (b) Extractive composition profile map at $(F_E/V) = 0.5$

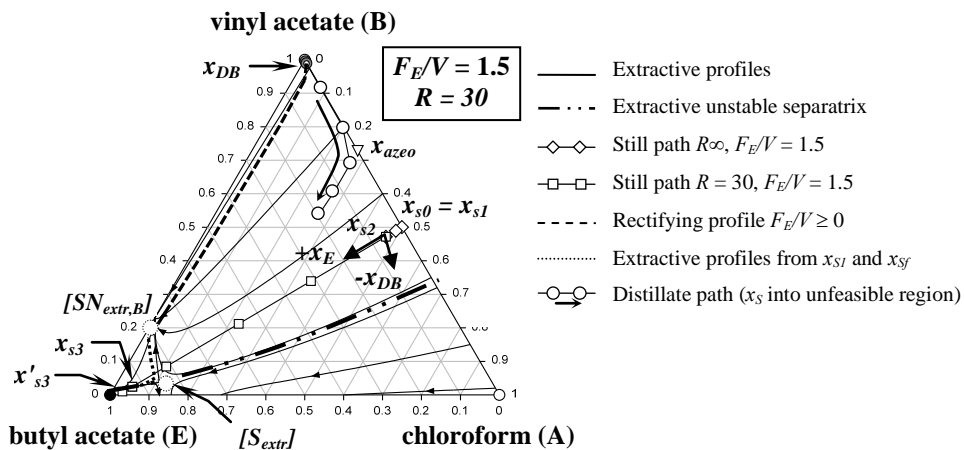


Figure 15. Extractive composition profile map and simulation results for $F_E/V = 1.5$ and $R = 30$.

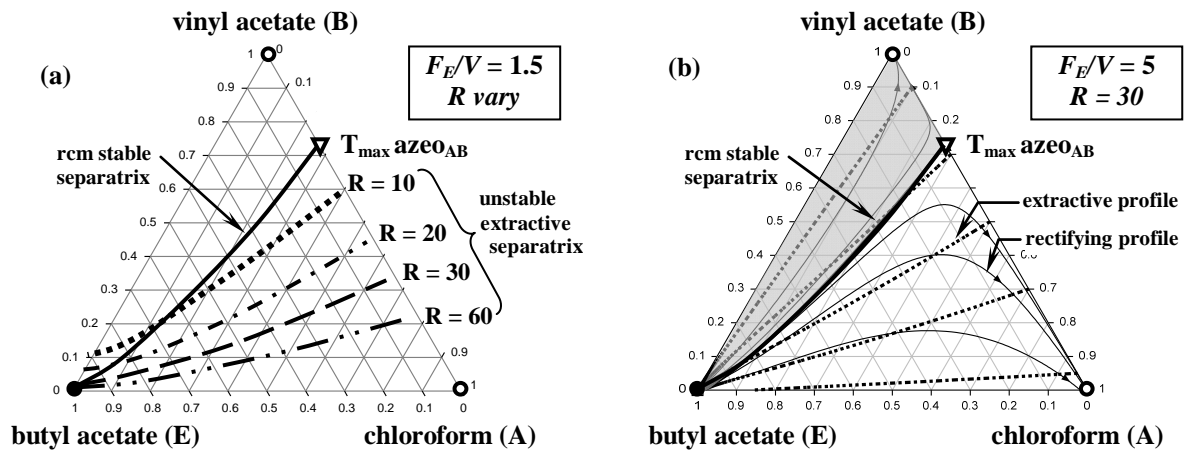


Figure 16. Influence of R and F_E/V on the feasible region to recover x_{DB} .

TABLE CAPTION

Table 1. Ternary Diagrams for Homogeneous Extractive Distillation (Serafimov's classification)

Entrainer	Minimum Boiling Azeotrope	Maximum Boiling Azeotrope	Low Volatility Mixtures
Light	1.0-2	1.0-1a	
Intermediate		1.0-1b	0.0-1
Heavy	1.0-1a	1.0-2	

Table 2. Binary coefficients for computing the ternary liquid – vapour equilibrium

Binary Coefficients [cal/mol]	Model	A_{ij}	A_{ji}	α_{ij}
Acetone (A) – Heptane (B)		881.932	297.031	0.2892
Acetone (A) – Toluene (E)	NRTL	276.942	81.9727	0.3010
Heptane (B) – Toluene (E)		-84.9143	436.388	0.3895
Acetone (A) – Methanol (B)		184.701	222.645	0.3084
Acetone (A) – Chlorobenzene (E)	NRTL	860.409	-328.06	0.3000
Methanol (B) – Chlorobenzene (E)		860.712	1242.60	0.4690
Acetone (A) – Chloroform (B)		-643.277	228.457	0.3043
Acetone (A) – Benzene (E)	NRTL	-193.340	569.931	0.3007
Chloroform (B) – Benzene (E)		57.4140	-144.355	0.3038
Chloroform (A) – vinyl acetate (B)				
Chloroform (A) – Butyl acetate (E)	UNIFAC			
Vinyl acetate (B) – Butyl acetate (E)				